



HAL
open science

Origin and abundance of water in carbonaceous asteroids

Yves Marrocchi, David V Bekaert, Laurette Piani

► **To cite this version:**

Yves Marrocchi, David V Bekaert, Laurette Piani. Origin and abundance of water in carbonaceous asteroids. *Earth and Planetary Science Letters*, 2018, 482, pp.23-32. 10.1016/j.epsl.2017.10.060 . hal-02357542

HAL Id: hal-02357542

<https://hal.univ-lorraine.fr/hal-02357542>

Submitted on 10 Nov 2019

HAL is a multi-disciplinary open access archive for the deposit and dissemination of scientific research documents, whether they are published or not. The documents may come from teaching and research institutions in France or abroad, or from public or private research centers.

L'archive ouverte pluridisciplinaire **HAL**, est destinée au dépôt et à la diffusion de documents scientifiques de niveau recherche, publiés ou non, émanant des établissements d'enseignement et de recherche français ou étrangers, des laboratoires publics ou privés.

Origin and abundance of water in carbonaceous asteroids

Yves Marrocchi*, David V. Bekaert and Laurette Piani

CRPG, CNRS, Université de Lorraine, UMR 7358, Vandoeuvre-les-Nancy, F-54501, France

*Corresponding author: yvesm@crpg.cnrs-nancy.fr

Abstract

The origin and abundance of water accreted by carbonaceous asteroids remains underconstrained, but would provide important information on the dynamic of the protoplanetary disk. Here we report the *in situ* oxygen isotopic compositions of aqueously formed fayalite grains in the Kaba and Mokoia CV chondrites. CV chondrite bulk, matrix and fayalite O-isotopic compositions define the mass-independent continuous trend ($\delta^{17}\text{O} = 0.84 \pm 0.03 \times \delta^{18}\text{O} - 4.25 \pm 0.1$), which shows that the main process controlling the O-isotopic composition of the CV chondrite parent body is related to isotopic exchange between ^{16}O -rich anhydrous silicates and ^{17}O - and ^{18}O -rich fluid. Similar isotopic behaviors observed in CM, CR and CO chondrites demonstrate the ubiquitous nature of O-isotopic exchange as the main physical process in establishing the O-isotopic features of carbonaceous chondrites, regardless of their alteration degree. Based on these results, we developed a new approach to estimate the abundance of water accreted by carbonaceous chondrites (quantified by the water/rock ratio) with CM (0.3-0.4) \geq CR (0.1–0.4) \geq CV (0.1–0.2) $>$ CO (0.01–0.10). The low water/rock ratios and the O-isotopic characteristics of secondary minerals in carbonaceous chondrites indicate they (i) formed in the main asteroid belt and (ii) accreted a locally derived (inner Solar System) water formed near the snowline by condensation from the gas phase. Such results imply low influx of D- and ^{17}O - and ^{18}O -rich water ice grains from the outer part

34 of the Solar System. The latter is likely due to the presence of a Jupiter-induced gap in the
35 protoplanetary disk that limited the inward drift of outer Solar System material at the
36 exception of particles with size lower than 150 μm such as presolar grains. Among
37 carbonaceous chondrites, CV chondrites show O-isotopic features suggesting potential
38 contribution of $^{17-18}\text{O}$ -rich water that may be related to their older accretion relative to other
39 hydrated carbonaceous chondrites.

40
41
42
43
44
45
46
47
48
49
50
51
52
53
54
55
56
57
58
59
60
61
62
63
64
65
66
67
68
69
70
71
72
73
74
75
76
77

Highlights

- Bulk, matrix and fayalite grains of CV chondrites define a continuous trend.
- O-isotopic compositions of C-rich asteroids are established by isotopic exchange.
- We estimated the abundance of water accreted by carbonaceous chondrites.
- Carbonaceous asteroids formed in the asteroid belt and accreted local water.
- Our results support low influx of ^{17}O - and ^{18}O -rich water ice from the outer Solar System.

Keywords: carbonaceous asteroids, water, oxygen isotopes, protoplanetary disk, Jupiter.

78 **1- Introduction**

79

80

81

82 Water played a key role in shaping the Solar System as it account for about 50% by
83 mass of all condensable species in a gas of cosmic composition (Lodders, 2003). Water vapor
84 controls oxygen fugacity, affecting the chemistry of sub-millimeter materials formed during
85 the evolution of the solar protoplanetary disk. As bouncing and fragmentation limit the
86 coagulation of dust particles, the growth processes from dust to planetesimals are not fully
87 understood (Güttler et al., 2010). Water-ice mantling grain surfaces is believed to enhance
88 their adhesion and promote particle coagulation processes (Gundlach and Blum, 2015). Thus,
89 condensed water ices can locally increase the abundance of solids, favoring conditions that
90 trigger streaming instabilities, and allowing the growth of decimeter-sized pebbles that can
91 accrete to form planetesimals (Ros and Johansen, 2013). Water ice is thus fundamental to the
92 evolution of the Solar System, and, alongside oxides, silicates and metal, likely represented a
93 significant fraction of the building blocks of planets. Ice-free chondrite accretion likely took
94 place during the evolution of the protoplanetary disk as attested by enstatite chondrites, which
95 show really limited traces of water (Brearley, 2006; Piani et al., 2011).

96 Within the solar protoplanetary disk, the formation of water ice is mainly controlled

97 by the snowline, i.e., the distance from the Sun at which temperature is low enough for water

98 to condense (about 150-170 K). The location of the snowline in the protoplanetary disk is a

99 direct function of the stellar accretion rate and is expected to move inward as the accretion

100 rate decreases with time (Bitsch et al., 2015). Based on astronomical observations, stellar

101 accretion rates are estimated to have decreased on average from $10^{-8} M_{\odot}/y$ at 1 My to $1-5 \cdot 10^{-9}$

102 M_{\odot}/y at 3 My (M_{\odot} = the solar mass $\sim 2 \cdot 10^{30}$ kg) (Hartmann et al., 1998), inducing the

103 snowline to drift from 3 AU to 1 AU (astronomical unit AU = 150×10^6 km, the distance

104 from Earth to the Sun) (Bitsch et al., 2015). Such a snowline drift implies that water ice grains

were ubiquitous in the inner Solar System, and formed abundant ice-rich planetesimals. This

105 point is not insignificant as geochemical constraints and numerical simulations suggest that
106 inner planetesimals should have grown "dry" with only a small contribution of ice-rich
107 planetesimals originating from larger heliocentric distances (Albarède, 2009; Marty, 2012).
108 Yet, the accretion of chondrites occurred ~2–4 My after the formation of Calcium-
109 Aluminum-rich Inclusions (CAIs; Sugiura and Fujiya, 2014), when the snowline should have
110 been closer to the Sun than the inner edge of the asteroid belt (Morbidelli et al., 2016). Such a
111 conundrum, referred as the snowline problem (Oka et al., 2011), could be linked to inhibited
112 water ice condensation due to the slower drift of the snowline than that of gas in the
113 protoplanetary disk (Morbidelli et al., 2016). This would bring "dry" gas (from which water
114 had already condensed farther out in the disk) in the vicinity of the snowline (Morbidelli et al.,
115 2016). However, chondrites have been affected by variable but widespread water alteration
116 processes, suggesting they accreted a significant amount of water ice (Doyle et al., 2015;
117 Garenne et al., 2014; Vacher et al., 2017). Thus, the origin and the abundance of water
118 accreted by different group of chondrites are not yet fully understood (Alexander, 2017;
119 Vacher et al., 2016). Additionally, the oxygen isotopic evolution of water during secondary
120 alteration processes has not been fully investigated, and could provide invaluable information
121 on the physico-chemical processes occurring during the geological evolution of carbonaceous
122 asteroids (Clayton and Mayeda, 1999; 1984).

123 Oxygen isotopic compositions are expressed in delta units (‰) relative to Standard
124 Mean Ocean Water (SMOW) as $\delta^x\text{O} = [({}^x\text{O}/{}^{16}\text{O})_{\text{sample}}/({}^x\text{O}/{}^{16}\text{O})_{\text{SMOW}} - 1] \times 1000$ with x being
125 ${}^{17}\text{O}$ or ${}^{18}\text{O}$; mass-independent oxygen isotope fractionation are described by the parameter
126 $\Delta^{17}\text{O} = \delta^{17}\text{O} - 0.52 \times \delta^{18}\text{O}$. Among meteorites, carbonaceous chondrites present the most
127 widespread evidences of fluid-rock interactions, in that they contain important diversity of
128 aqueously formed minerals such as phyllosilicates, carbonates and magnetite (Brearley,
129 2006). Oxygen isotopic compositions of these secondary minerals can be used to decipher the

130 origin of water in the chondrite-forming region as outer water ices are expected to exhibit
131 significant ^{17}O and ^{18}O enrichment ($\Delta^{17}\text{O} \gg 0$) relative to inner Solar System values ($\Delta^{17}\text{O} \approx$
132 0) due to the self-shielding of ^{16}O -rich nebular CO gas by UV light (Yurimoto and Kuramoto,
133 2004). In addition, oxygen isotopic compositions at both the bulk and mineral scales can be
134 used to quantify (i) the abundance of water accreted by carbonaceous parent bodies (Clayton
135 and Mayeda, 1984; Young et al., 1999) and (ii) the prevailing conditions during subsequent
136 fluid-rock (Verdier-Paoletti et al., 2017). Among secondary minerals, fayalite (Fe_2SiO_4) is of
137 primary importance as it represents a proxy of the fluid from which it formed due to its low
138 fractionation factor $\alpha_{\text{Fa-water}}$ (Zheng, 1993) at the temperature range estimated for fayalite
139 formation (i.e., 100-300°C) (Doyle et al., 2015; Zolotov et al., 2006). In this contribution, we
140 report the oxygen isotopic compositions of fayalite in the CV chondrites Kaba and Mokoia.
141 We compute the amount of water ice accreted by combining these results with the bulk O-
142 isotopic compositions of CV chondrites (Clayton and Mayeda, 1999). We also compare the
143 O-isotopic composition at both the bulk and (secondary) mineral scales for CO, CM and CR
144 chondrites to propose a quantitative view of the origin, abundance and O-isotopic evolution of
145 water in the carbonaceous asteroids.

146
147
148
149
150

2-Materials and methods

151 We surveyed a thin section each of Kaba (Kaba N4075) and Mokoia (Mokoia N1185;
152 both from the National Museum History, Vienna, Austria). Sections were examined
153 microscopically in transmitted and reflected light. Scanning electron microscope (SEM) and
154 Energy Dispersive X-ray (EDX) spectral analyses were performed at Centre de Recherches
155 Pétrographiques et Géochimiques (CRPG-CNRS, Nancy, France) using a JEOL JSM-6510
156 equipped with an EDX Genesis X-ray detector, using a 3 nA primary beam at 15 kV.
157 Quantitative compositional analyses of fayalite were made with a CAMECA SX-100 electron

158 microprobe at the University of Paris VI. Electron microprobe analyses of silicates were
159 performed with a 40 nA focused beam, 15 kV accelerating potential, and 20 on-peak and
160 background analysis times. Detection limits in silicates were 0.02 wt% for SiO₂, Al₂O₃, CaO
161 and MgO, 0.01 wt% for Na₂O, K₂O, and TiO₂, and 0.04 wt% for Cr₂O₃ and FeO.

162 Oxygen isotopic compositions were measured with a CAMECA IMS 1280 at CRPG-
163 CNRS. ¹⁶O⁻, ¹⁷O⁻, and ¹⁸O⁻ ions produced by a 5 nA Cs⁺ primary ion beam were measured in
164 multi-collection mode with three Faraday cup (FC). To avoid interference of ¹⁶OH⁻ and ¹⁷O⁻
165 signals at mass 17, and to maximize the flatness of the ¹⁶O⁻ and ¹⁸O⁻ peaks, entrance and exit
166 slits were adjusted to achieve a Mass Resolving Power of ~7000 for ¹⁷O⁻ on the central FC
167 and ~2500 on the off-axis FC. Total measurement time was 240 s (180 s measurement + 60 s
168 pre-sputtering). We used four terrestrial standard materials (San Carlos olivine, magnetite,
169 diopside, and fayalite) to: (i) define the mass fractionation line (TFL) and (ii) correct the
170 matrix effects on instrumental mass fractionation for fayalite. Typical count rates obtained on
171 fayalite grains were 3 × 10⁹ cps for ¹⁶O, 1 × 10⁶ cps for ¹⁷O, and 4.5 × 10⁶ cps for ¹⁸O. Typical
172 2σ errors were ~ 0.7 ‰ for δ¹⁸O, ~ 0.8 ‰ for δ¹⁷O, and ~ 1 ‰ for Δ¹⁷O.

173 **3-Results**

174
175
176
177 Fayalite grains in Kaba and Mokoia occur in peripheral portions of type I chondrules,
178 in fine-grained chondrule rims, and in matrix (Fig. 1). Fayalite are large, subhedral-to-
179 anhedral grains, and sometimes associated with magnetite and sulfide grains (Fig. 1A),
180 although sulfide- and magnetite-free fayalite grains are commonly observed in the matrix
181 (Fig. 1B). Fayalite are chemically homogeneous (Fa₉₇ to Fa₁₀₀; Table 1) with compositions
182 similar to those previously reported fayalite-bearing assemblages (Choi et al., 2000; Hua and
183 Buseck, 1995; Jogo et al., 2009). Eight large (> 40 μm) sulfide- and magnetite-free fayalite

184 grains were selected for isotopic analyses. Their O-isotopic compositions fall above the TFL,
185 with $\Delta^{17}\text{O}$ values ranging from 0.8 to 2.6‰ (Fig. 2, Table 2).

186
187
188
189
190

4-Discussion

4.1 Origin, abundance and O-isotopic evolution in CV chondrites

191
192
193
194

It is commonly accepted that bulk O-isotopic compositions of CV chondrites plot
195 along the Carbonaceous Chondrite Anhydrous Mineral (CCAM) line [$\delta^{17}\text{O} = (0.94 \pm 0.01) \times$
196 $\delta^{18}\text{O} - 4.2$], derived from BrF_5 analyses of anhydrous minerals from CAIs in carbonaceous
197 chondrites (Clayton et al., 1973). In detail, it rather appears that bulk and matrix O-isotopic
198 compositions of CV chondrites define the trend $\delta^{17}\text{O} = 0.84 \times \delta^{18}\text{O} - 4.25$ ($r^2 = 0.99$; Fig. 2A;
199 (Clayton and Mayeda, 1999; Greenwood et al., 2010), which likely corresponds to secondary
200 alteration processes. The O-isotopic compositions of fayalite grains reported here do not fall
201 on the TFL but show $\Delta^{17}\text{O} > 0\text{‰}$ (Fig. 2B). When plotted with the bulk, matrix and dark
202 inclusions O-isotopic compositions of CV chondrites, the Kaba and Mokoia fayalite grains
203 define the continuous trend $\delta^{17}\text{O} = (0.83 \pm 0.02) \times \delta^{18}\text{O} - (4.18 \pm 0.13)$ (2σ , $r^2 = 0.99$, and
204 Mean Squared Weight Deviation, MSWD = 3.9; Fig. 2A). Fayalite grains reported in the CV3
205 chondrite A-881317 also fall on this trend (Fig. 2A) (Doyle et al., 2015). Comparison with
206 other studies is difficult due to the large uncertainties associated with O-isotope
207 measurements (e.g., 4.4 and 2.5‰ on $\delta^{18}\text{O}$ and $\delta^{17}\text{O}$ (2σ), respectively) (Choi et al., 2000).
208 However, recent measurements in the Kaba chondrite aligns perfectly along the line of slope
209 0.83 (Fig. 2A; Krot and Nagashima, 2016). The continuous trend defined by bulk, matrix and
210 fayalite compositions does not follow a mass-dependent fractionation relationship (Fig. 2A),
211 implying that fayalite O-isotopic compositions did not result from fluid circulation along a
212 temperature gradient, which would produce a trend with slope 0.52. Instead, this implies that

213 the main process controlling the O-isotopic composition of the CV chondrite parent body is
214 related to isotopic equilibrium between ^{16}O -rich anhydrous silicates and ^{17}O - and ^{18}O -rich
215 fluid as recently reported in CM chondrites (Verdier-Paoletti et al., 2017). In such a scheme,
216 ^{17}O - and ^{18}O -rich fayalite correspond to early precipitates from primitive fluids that did not
217 suffer significant O-isotopic exchange with ^{16}O -rich anhydrous silicates (Yurimoto et al.,
218 2014; Zolensky et al., 2017). Conversely, lighter isotopic compositions indicate that fayalite
219 formed only after significant alteration, as fluid O-isotopic compositions converge toward the
220 typical ^{16}O -rich values of anhydrous silicates. Both bulk and mineral phase data (Fig. 2) thus
221 identify O-isotopic exchange between ^{16}O -rich silicates and ^{17}O - and ^{18}O -rich fluid as the key
222 process controlling the O-isotopic composition of the alteration fluids from which fayalite
223 precipitated.

224 Thermodynamic calculations suggest that nearly pure fayalite grains ($\text{Fa} > 90$) as
225 observed in CV3_{OxB} chondrites are stable at temperatures below 350°C (Zolotov et al., 2006),
226 and likely down to 100-200°C (Doyle et al., 2015). Considering the low $\alpha_{\text{Fa-water}}$ at this
227 temperature range (i.e., $1000 \ln \alpha_{\text{Fa-water}} = -3.4 \text{‰}$ at 100°C and -1.1‰ at 200°C,
228 (Zheng, 1993), fayalite O-isotopic compositions represent a direct record of the oxygen
229 isotopic compositions of the fluid from which they precipitated. Additionally, fayalite and
230 magnetite from chondrite A-881317 lie on a mass-dependent fractionation line with $\Delta^{17}\text{O} =$
231 -0.3‰ , consistent with equilibrium crystallization from the same fluid reservoir (Fig. 3B)
232 (Doyle et al., 2015). The -8.4‰ difference between $\delta^{18}\text{O}$ values of fayalite and magnetite
233 (Doyle et al., 2015) corresponds to fayalite crystallization at $\approx 150^\circ\text{C}$ (Zheng, 1993), at which
234 temperature the fractionation factor α is minimal with $1000 \ln \alpha_{\text{Fa-water}} \approx 0.6 \text{‰}$.
235 Considering then that fayalite formation likely occurred in a very narrow range of
236 temperatures (i.e., 150-200°C), their parent fluids are characterized by near terrestrial values
237 with $\Delta^{17}\text{O}$ from -1 to $+3.5\text{‰}$ (Fig. 2A). However, these values do not necessarily correspond

238 to the initial O-isotopic composition of water accreted by CV chondrites as protracted fluid-
239 rock interactions likely occurred before the precipitation of the rare, nearly pure, fayalite
240 grains.

241 There is a lively debate on the conditions of secondary alteration processes that have
242 affected chondrites, which is basically divided into open-system (Young et al., 1999) versus
243 closed-system models (Clayton and Mayeda, 1999). Although the O-isotopic compositions of
244 secondary minerals have been used to argue for both models, petrographic observations
245 appear more consistent with closed-system alteration. For instance, there is little evidence for
246 the redistribution of soluble elements within chondrites at scale greater than 100 μm (Brearley,
247 2006), thus suggesting that aqueous alteration processes are mostly isochemical. This is
248 consistent with the estimated low permeability of chondrites (Bland et al., 2009) and the lack
249 of variations in bulk chemical compositions between meteorites with different degrees of
250 aqueous alteration (Brearley, 2006). Based on these observations, we thus considered a
251 closed-system model to discuss the alteration conditions of carbonaceous asteroids.

252 In a closed system, the difference between the final (f) oxygen isotopic composition of
253 rock r and water w can be described as:

254

$$255 \quad \Delta = \delta_r^f - \delta_w^f \quad (1)$$

256

257

258 The amount of water accreted by CV chondrites can be estimated by the water/rock ratio
259 (Young et al., 1999)

260

261
$$\frac{N_w}{N_r} = \frac{(\delta_r^f - \delta_r^0)}{\delta_w^0 - (\delta_r^f - \Delta)} \quad (2)$$

262 where N corresponds to the number of oxygen atoms in the reacting water (w) or rock (r), δ^0
 263 their initial isotopic compositions, δ^f their final isotopic compositions and Δ represent the
 264 difference between rock and water at equilibrium. Such a formalism does not include the final
 265 isotopic composition of the water, which is generally not known. However, in the case where
 266 this parameter can be calculated, Eqn. 2 simplifies to:

267

268
$$\frac{N_w}{N_r} = \frac{(\delta_r^f - \delta_r^0)}{(\delta_w^0 - \delta_w^f)} \quad (3)$$

269

270 Considering the bulk O-isotopic composition of Kaba ($\delta^{18}\text{O} = 2.18\text{‰}$, (Clayton and Mayeda,
 271 1999) and a more ^{16}O -rich bulk CV chondrite as a plausible CV protolith ($\delta^{18}\text{O} = -4.22\text{‰}$;
 272 (Clayton and Mayeda, 1999), we calculate the water/rock ratio by assuming that the lowest
 273 $\delta^{18}\text{O}$ value of fayalite represent the final O-isotopic composition of CV water, after weighting
 274 by the fractionation factor at 150°C (i.e., $17.4 - 0.6 = 16.8\text{‰}$; Table 2). Although the initial
 275 composition of water accreted by CV chondrite is unknown, it must be (i) located on the trend
 276 defined by both bulk CV and fayalite (Fig. 2A) and (ii) characterized by $\delta^{18}\text{O}$ value higher
 277 than the highest fayalite $\delta^{18}\text{O}$ value. Assuming an initial water with $\delta^{18}\text{O} = 30\text{‰}$ (as estimated
 278 for CM chondrites; (Clayton and Mayeda, 1984) leads to an estimated water/rock ratio of 0.48
 279 for Kaba; the same calculation giving a result of 0.74 for Mokoia. These values are slightly
 280 lower than those estimated on the basis of mineral assemblages and thermodynamic modeling
 281 (i.e., 0.8–1.1; (Zolensky et al., 1993) However, it is noted that our estimations represent
 282 maximum water/rock ratios, as increasing the $\delta^{18}\text{O}$ of the initial water or decreasing $\delta^{18}\text{O}$ of

283 final water lowers the water/rock ratio. For instance, an initial water with $\delta^{18}\text{O} = 45\text{‰}$ gives
284 estimated water/rock ratios for Kaba and Mokoia of 0.30 and 0.22, respectively. Considering
285 the range of water/rock ratios modeled for the formation of near pure fayalite (i.e., 0.1-0.2;
286 (Zolotov et al., 2006) provides $\delta^{18}\text{O} \geq + 60 \text{‰}$ (i.e., $\Delta^{17}\text{O} > 15 \text{‰}$) for the initial CV water,
287 suggesting a potential contribution of water ice from the outer Solar System (Sakamoto et al.,
288 2007; Seto et al., 2008).

289 Kaba is considered the least altered oxidized CV chondrite with a petrographic grade
290 of 3.1-3.4 (Bonal et al., 2006). Interestingly, Kaba fayalite grains are not in isotopic
291 equilibrium with sulfide-associated magnetite (SAMs) poikilitically enclosed in low-Ca
292 pyroxenes of chondrules (Fig. 3; (Marrocchi et al., 2016). Based on petrographic and isotopic
293 characteristics, SAMs have been interpreted as magmatic minerals, resulting from the
294 crystallization of FeS melts containing variable amounts of dissolved oxygen (Marrocchi et
295 al., 2016; Marrocchi and Libourel, 2013). The fact that the $\Delta^{17}\text{O}$ of SAMs and fayalite grains
296 from Kaba do not overlap (Fig. 3B) confirms that chondrule SAMs could be primary mineral
297 formed during the high-temperature chondrule-forming event (Marrocchi et al., 2016). This
298 does not exclude the potential occurrence of low-temperature aqueously formed magnetite in
299 CV chondrites, but rather suggests that both processes occurred at different settings and under
300 different physico-chemical conditions.

301
302
303
304

4.2 Comparison of CV to CM, CR and CO chondrites

305 *4.2.1 CM chondrites*

306

307 In a oxygen three-isotope plot, the continuous trend observed between whole rocks
308 and secondary minerals is not unique to CV chondrites. In CM chondrites, Ca-carbonates
309 replace fayalite as aqueously formed minerals defining the trend $\delta^{17}\text{O} = (0.66 \pm 0.05) \times \delta^{18}\text{O} -$

310 (4.7 ± 1.5) (Verdier-Paoletti et al., 2017). This implies that isotopic equilibrium between ^{16}O -
311 rich anhydrous silicates and ^{17}O - and ^{18}O -rich water controls the O-isotopic evolution of bulk
312 CM chondrites and their secondary alteration mineral. To the first order, isotopic equilibrium
313 dominates, with temperature gradients having a lesser effect in establishing the isotopic
314 composition of CV and CM chondrites. Consequently, the isotopic compositions of secondary
315 minerals are mainly controlled by the extent of isotopic exchange between water of initial
316 composition and anhydrous silicates (Clayton and Mayeda, 1984; Verdier-Paoletti et al.,
317 2017). In such a scheme, ^{17}O - and ^{18}O -rich secondary minerals correspond to early
318 precipitates from primitive fluids that had not yet suffered significant O-isotopic exchange
319 with anhydrous silicates.

320 In CM chondrites, the O-isotopic compositions of alteration water inferred from direct
321 measurements and mass balance calculations define a continuous trend, parallel within errors
322 to that of bulk CMs and Ca-carbonates, but with a different intercept ($\delta^{17}\text{O} = (0.69 \pm 0.02) \times$
323 $\delta^{18}\text{O} - (2.12 \pm 0.30)$); (Verdier-Paoletti et al., 2017). This difference in intercepts is directly
324 related to the isotopic fractionation factor, reflecting an average calculated precipitation
325 temperature of 110°C for CM Ca-carbonates (Verdier-Paoletti et al., 2017). Similarly, Ca-
326 carbonates of the Murchison and Mighei CM chondrites define a trend parallel to the CM
327 water line, but with an intercept in good agreement, within errors, to that reported for 9
328 different CM chondrites ($\delta^{17}\text{O} = (0.70 \pm 0.03) \times \delta^{18}\text{O} - (5.65 \pm 1.25)$) (Fig. 4A: (Lindgren et al.,
329 2017; Verdier-Paoletti et al., 2017). Such results allow calculation of the O-isotopic
330 composition of the fluid from which a given carbonate precipitated by connecting the Ca-
331 carbonate trend to the CM water line by a mass-dependent line (see (Verdier-Paoletti et al.,
332 2017) for further details). Using the bulk O-isotopic composition of Murchison and Mighei
333 (i.e., 7.3 and 7.6‰, respectively; (Clayton and Mayeda, 1999) and the O-isotopic composition
334 of anhydrous CM silicates as plausible CM protolith (i.e., $\delta^{18}\text{O} = -4.2\text{‰}$; (Clayton and

335 Mayeda, 1999), we calculate the water/rock ratio (Eqn. 3) assuming that the lowest Ca-
336 carbonate $\delta^{18}\text{O}$ value in a given CM chondrite represent the final $\delta^{18}\text{O}$ value of water
337 (weighted by 14.6‰, representing $1000 \ln \alpha_{\text{calcite-water}}$ at 110°C). Murchison and Mighei thus
338 show water/rock ratios of 0.32 and 0.36, respectively, in good agreement with previous
339 estimates for CM2 chondrites (i.e., 0.3-0.6; (Clayton and Mayeda, 1984; Zolensky et al.,
340 1997).

341 With the exception of few Ca-carbonates enriched in ^{17}O - and ^{18}O relative to the main
342 carbonate trend (Vacher et al., 2016), the O-isotopic characteristics of secondary mineral in
343 CM chondrites indicate a dominant local origin of water during accretion (Alexander et al.,
344 2012). Near terrestrial $\Delta^{17}\text{O}$ values of the CM water line (-1 to + 4 ‰; Fig. 4B) confirm a
345 local water origin. Consequently, the contribution in CM chondrites of water coming from
346 large heliocentric distances is probably limited to few %. Such contributions could have been
347 overprinted by water inherited from the inner Solar System, as indicated by the hydrogen
348 isotopic composition of CM chondrites (Piani et al., 2017).

349
350 *4.2.2 CR chondrites*
351

352 Of the carbonaceous chondrites, CR chondrites are of primary importance because
353 they exhibit low degree of aqueous alteration and thermal metamorphism (Le Guillou and
354 Brearley, 2014). Nonetheless, they experienced significant alteration as attested by the
355 corrosion of Fe-Ni metal beads (Morlok and Libourel, 2013) and the presence of Ca-
356 carbonates (Brearley, 2006). Interestingly, CR chondrites show similar O-isotopic
357 characteristics as CV and CM chondrites, with bulk and Ca-carbonates O-isotopic
358 compositions defining the trend with $\delta^{17}\text{O} = (0.63 \pm 0.02) \times \delta^{18}\text{O} - (2.22 \pm 0.26)$ (Fig. 5A;
359 (Clayton and Mayeda, 1984; Jilly, 2015; Schrader et al., 2011). This similarity attests the

360 ubiquitous nature of O-isotopic exchange as the main physical process controlling the O-
361 isotopic compositions of carbonaceous chondrites, whatever the extent of alteration.

362 Magnetite in CR chondrites is sometimes in close association with Ca-carbonates
363 (Brearley, 2006; Jilly, 2015). Within a given CR chondrite, the two fall on a mass-dependent
364 line (e.g., GRO 95577; Fig. 5B) with $\Delta^{17}\text{O} \sim 0$ ‰ (Jilly, 2015; Jilly et al., 2014), indicating
365 that they probably formed at isotopic equilibrium from the same fluid reservoir. Assuming
366 such equilibrium, the fractionation factor between carbonates (cc) and magnetite (mt) $\Delta^{18}\text{O}_{\text{mt-cc}}$
367 (i.e., $\delta^{18}\text{O}_{\text{mt}} - \delta^{18}\text{O}_{\text{cc}}$) is a function of their formation temperature (Chacko et al., 2001):

368

$$369 \quad \Delta^{18}\text{O}_{\text{mt-cc}} = (-2.10 \times 10^{-4} \text{ T}^{-2}) + (0.12 \text{ T}) - 34.46 \quad (4)$$

370

371 Based on data from different CR chondrites (Jilly, 2015), this calculation provides a
372 formation temperature estimate of 15–110°C, in good agreement with previous estimations of
373 50–150°C (Zolensky et al., 1993). At those temperature, we compute the O-isotopic
374 compositions of water from which carbonates and magnetite formed in the different CR
375 chondrites (Jilly, 2015; Jilly et al., 2014). CR water thus (i) defines a trend with $\delta^{17}\text{O} = (0.61$
376 $\pm 0.03) \times \delta^{18}\text{O} + (0.42 \pm 0.15)$ (Fig. 6A) and (ii) is characterized by $\Delta^{17}\text{O} \sim 0$ ‰, consistent
377 with water originating from the inner Solar System. Interestingly, the CR water trend
378 estimated from the O-isotopic compositions of Ca-carbonates and magnetite perfectly aligns
379 with the estimation of the O-isotopic composition of water accreted by CM chondrites
380 (Clayton and Mayeda, 1999; 1984) (Fig. 5A). This suggests that both types of chondrites
381 could have accreted similar water, implying that the $\delta^{17}\text{O}$ and $\delta^{18}\text{O}$ values of initial CM water
382 could be used to estimate the CR chondrite W/R ratios.

383 Definition of the CR water line allows calculation of the O-isotopic composition of the
384 specific fluid from which a given CR carbonate precipitated, as their respective O-isotopic

385 compositions are related by a mass-dependent relationship. This further allows estimation of
386 the water/rock ratio by assuming that (i) the lowest O-isotopic composition of bulk CR
387 chondrites represent the $\delta^{18}\text{O}$ of the CR protolith (i.e., -2.29‰; Fig. 5A; (Schrader et al.,
388 2011) and (ii) the initial CR water is similar to that accreted by CM chondrites (i.e., 30‰;
389 (Clayton and Mayeda, 1984). This leads to a maximum estimation of the CR water/rock ratio
390 in the range 0.10 to 0.40, lower than previous values of 0.4-1.1 (Zolensky et al., 1993).

391
392 *4.2.3 CO chondrites*

393
394
395 The case of CO chondrites is more complex than other carbonaceous chondrites. First,
396 CO chondrites have experienced minimal fluid alteration; some show no evidence of
397 alteration, whereas others exhibit alteration features at the sub-micrometer scale (Brearley,
398 2006). Rare secondary phases (phyllosilicates, fine-grained serpentine and saponite) are
399 mainly located within the CO matrices (Brearley, 2006). Secondly, the bulk O-isotopic
400 compositions of CO chondrite finds could have been affected by terrestrial weathering,
401 inducing a shift toward ^{17}O - and ^{18}O -rich values (Greenwood and Franchi, 2004). Finally, a
402 recent report of the bulk O-isotopic composition of CO chondrite falls show they are slightly
403 shifted toward the CCAM line (Alexander et al., 2017) relative to previous measurements
404 (Clayton and Mayeda, 1999; Greenwood and Franchi, 2004) (Fig. S1). The reason for such a
405 shift remains unclear but could be linked to incomplete fluorination in previous measurements
406 (Alexander et al., 2017). However, several observations can be used to improve our
407 understanding of CO chondrites. (i) Considering the data reported by (Clayton and Mayeda,
408 1999; Greenwood and Franchi, 2004), the bulk O-isotopic compositions of CO chondrite falls
409 show a significant deviation from the primordial slope 1 with $\delta^{17}\text{O} = (0.65 \pm 0.12) \times \delta^{18}\text{O} -$
410 (4.19 ± 0.27) (Fig. 6A; $r^2 = 0.89$, MSWD = 7.6). (ii) This trend is similar to the one defined
411 by CM chondrites (Fig. 6A). Although recent report suggest that CM and CO chondrites

412 could originate from distinct parent bodies (Schrader and Davidson, 2017), they probably
413 formed in a common region within the accretion disk; the anhydrous precursors of CM2 were
414 CO3-like, but CM accreted more water (Hewins et al., 2014). (iii) Taken together, the CM
415 and CO falls define a trend with $\delta^{17}\text{O} = (0.69 \pm 0.04) \times \delta^{18}\text{O} - (4.05 \pm 0.18)$ (Fig. 6A; $r^2 =$
416 0.98 , MSWD = 15). Although the bulk O-isotopic compositions of CO chondrites are more
417 restricted than those of CM chondrites (Fig. 6a), they might have recorded fluid alteration
418 processes. (iv) The absence of secondary phases that could be targeted by ion probe
419 measurements precludes the possibility of combining bulk and mineral data (as reported for
420 CV, CM and CR chondrites). However, MacAlpine Hills (MAC) 88107, a CO-like chondrite,
421 shows abundant near-pure fayalite and magnetite (Krot et al., 2000) that can be used to
422 estimate the isotopic characteristics of CO water. The O-isotopic compositions of fayalite
423 from MAC 88107 fall along the trend defined by the bulk CM and CO chondrites, $\delta^{17}\text{O} =$
424 $(0.69 \pm 0.03) \times \delta^{18}\text{O} - (4.01 \pm 0.21)$ (Fig. 6A; $r^2 = 0.98$, MSWD = 15). These observations
425 suggest that the O-isotopic characteristics of CO chondrites were established by O-isotopic
426 exchange between anhydrous silicates and significantly less water than the other groups of
427 carbonaceous chondrites.

428 Magnetite and fayalite in MAC 88107 plot along a mass-dependent fractionation line
429 with $\delta^{17}\text{O} = (0.48 \pm 0.02) \times \delta^{18}\text{O} - (1.10 \pm 2.05)$ (Fig. 6B; $r^2 = 0.84$, MSWD = 0.56),
430 interpreted as formation at isotopic equilibrium with the same fluid reservoir (Doyle et al.,
431 2015). Based on O-isotopic compositions and mineralogical, petrographic and
432 thermodynamic constraints, it has been proposed that fayalite and magnetite formed at low
433 water/rock ratios (0.1–0.2) and relatively elevated temperature (100–200°C; (Doyle et al.,
434 2015). However, considering the average $\delta^{18}\text{O}$ values of magnetite and fayalite (i.e., $10.2 \pm$
435 1.3‰ and $14.1 \pm 0.6\text{‰}$, respectively), the observed $\Delta^{18}\text{O}_{\text{mt-Fa}}$ ($= \delta^{18}\text{O}_{\text{mt}} - \delta^{18}\text{O}_{\text{Fa}}$) rather
436 suggests a formation temperature of $480 \pm 20^\circ\text{C}$ (Chacko et al., 2001). Considering even the

437 larger $\Delta^{18}\text{O}_{\text{mt-Fa}}$ (Doyle et al., 2015) leads to an estimate temperature of $\sim 250^\circ\text{C}$, significantly
438 higher than that previously estimated for CO chondrites (i.e., $0\text{--}50^\circ\text{C}$) (Zolensky et al., 1993).
439 Whatever the alteration temperature of MAC 88107, the fractionation factor $\alpha_{\text{Fa-water}}$ is
440 relatively small (i.e., 3.4‰ at 100°C and -3.6‰ at 500°C) (Zheng, 1993), allowing the final
441 O-isotopic composition of CO water to be computed at $\delta^{18}\text{O}$ of $15 \pm 3.5\text{‰}$. Although the bulk
442 O-isotopic composition of MAC 88107 has not been determined, it is possible to estimate the
443 water/rock ratio of CO chondrites by following some reasonable assumptions. Considering
444 that MAC 88107 likely has a bulk O-isotopic composition falling in the lower range observed
445 for CO chondrites (i.e., -4 to -2‰) and assuming that COs have similar initial water and
446 anhydrous protolith as CMs ($+30.3$ and -4.2‰ , respectively; (Clayton and Mayeda, 1984),
447 the water/rock estimated for MAC 88107 range from 0.01 to 0.10. These values are consistent
448 with previous estimates (Zolensky et al., 1993) and the limited alteration of CO chondrites
449 relative to CV and CM. However, it should be kept in mind that the lack of secondary phases
450 in CO chondrites makes this estimation less robust than those reported for CM, CR and CV
451 chondrites.

452

453 **4.3 Implications for the structure and evolution of the accretion disk**

454

455 All carbonaceous chondrites show varying degrees of fluid alteration suggesting that
456 water ice grains were significant components of their parent bodies. By combining bulk and
457 mineral O-isotope data, we estimate the water/rock ratios of carbonaceous chondrites to be:
458 CM ($0.3\text{--}0.4$) \geq CR ($0.1\text{--}0.4$) \geq CV ($0.1\text{--}0.2$) $>$ CO ($0.01\text{--}0.10$) (Fig. 7). Our results suggest
459 that water was heterogeneously distributed across the chondrite accretion regions. Current
460 debate considers carbonaceous chondrites formation either in the main asteroid belt
461 (Alexander et al., 2012) or in the outer Solar System (i.e., $5\text{--}15$ UA) before subsequent
462 implantation into the main belt during the dynamic evolution of the Solar System (the Grand

463 Tack model; (Walsh et al., 2011). The low water/rock ratios estimated in this study support
464 carbonaceous chondrite accretion close to the snowline as accretion at greater heliocentric
465 distances would have induced a solar water/rock ratio of 1.2 (Lodders, 2003). The low
466 carbonaceous chondrite water/rock ratios suggest that the snowline did not drift closer to the
467 Sun than the inner edge of the asteroid belt (Morbidelli et al., 2016) and was probably located
468 at 2–3 AU during the accretion of the carbonaceous asteroid, ~2–4 My after the formation of
469 CAIs (Krot et al., 2015).

470 The majority of secondary minerals in carbonaceous chondrites show O-isotopic
471 signatures that are consistent with accretion of locally derived water from the inner Solar
472 System. Such water presents minimal mass-independent O-isotopic variations (i.e., $\Delta^{17}\text{O} \sim$
473 0‰), contrary to outer water ices enriched in ^{17}O - and ^{18}O ($\Delta^{17}\text{O} \gg 0\%$), implying that water
474 ice originating from the outer Solar System was not the main source for water in
475 carbonaceous chondrites (Yurimoto and Kuramoto, 2004). This conclusion is consistent with
476 D-poor compositions of carbonaceous chondrite waters (Alexander 2012, Piani 2017). Based
477 on the expected heliocentric D/H gradient ratio in the accretion disk (Jacquet and Robert,
478 2013), both H and O isotopes suggest an inner Solar System origin of water accreted into
479 carbonaceous chondrite, probably where carbonaceous asteroids are located today (Alexander,
480 2017).

481 The low influx of ^{17}O - and ^{18}O -rich and D-rich water ice from the outer part of the
482 Solar System may be due to the early growth of Jupiter ($\approx 1\text{My}$ after the start of the Solar
483 System), which would have prevented inward radial drift in the protoplanetary disk (Walsh et
484 al., 2011). An inner Solar System origin of carbonaceous chondrites is consistent with their
485 type I chondrules containing olivines with $\text{Mg}\# > 90$, suggesting formation at relatively low
486 oxygen fugacity, whereas formation beyond the orbit of Jupiter should have occurred under
487 more oxidizing conditions. Contrary to these conclusions, (Kruijer et al., 2017) attribute the

488 molybdenum and tungsten isotopic compositions of iron meteorites derived from a
489 carbonaceous meteorite reservoir to a late addition of W- and Mo-bearing presolar material to
490 the outer Solar System. However, presolar grains (generally $< 20 \mu\text{m}$ in size), being tightly
491 coupled to gas motions (i.e., particles $< 150 \mu\text{m}$ in size; Fig. 8C) might have crossed Jupiter's
492 orbit and reached the inner Solar System (Zhu et al., 2012). As the carrier phases of Mo and
493 W isotope anomalies (Kruijer et al., 2017), presolar grains could have thus been preferentially
494 incorporated into asteroids accreting near the snow line, i.e. carbonaceous chondrites (Fig.
495 8D). Chondrites forming at smaller heliocentric distances and/or earlier in the history of the
496 protoplanetary disk would have incorporated a different population of presolar grains.
497 Ordinary chondrites are consistent with such an origin, as their potential earlier onset of
498 aqueous activity (Krot et al., 2015; Sugiura and Fujiya, 2014) as well as D-rich water and
499 organic matter relative to carbonaceous chondrites (Piani et al., 2015) could have resulted
500 from accretion before the Jupiter-induced gap in the protoplanetary disk. Additionally,
501 ordinary chondrites contain more type II chondrules characterized by low Mg# olivines (i.e.,
502 $\text{Mg}\# < 90$) than carbonaceous chondrites, indicating their formation in more oxidizing
503 environments.

504 Carbonaceous chondrites and their water are thus by-products of the evolution of the
505 inner Solar System. The O-isotopic composition of water produced via self-shielding
506 photodissociation decreases with time and increasing heliocentric distance in the accretion
507 disk, becoming similar to that observed in carbonaceous chondrites after 1 My (Yang et al.,
508 2011). Consequently, the O-isotopic of water upon the accretion of hydrated carbonaceous
509 parent bodies (i.e., 2–4 Ma; (Sugiura and Fujiya, 2014) should have been smoothed toward
510 Earth-like values, potentially via re-equilibration with silicates in the disk (Alexander, 2017;
511 Yurimoto and Kuramoto, 2004). Inner solar water accreted by hydrated carbonaceous
512 asteroids may be ice condensed at the snow line and/or liquid water adsorbed at the grain

513 surfaces. The increasing water/rock ratios of CO, CV, CR, and CM reflects that these classes
514 of carbonaceous asteroids accreted near to the snow line, but at increasing heliocentric
515 distances. We note that some Ca-carbonates of the least altered CM chondrite Paris have
516 peculiar O-isotopic compositions suggesting accretion of few percent water ice grains
517 originating from the outer part of the Solar System (Vacher et al., 2016). This is supported by
518 the distinct C/H vs. D/H correlation reported for the Paris' matrix compared to the other CM
519 chondrites (Piani et al., 2017). These results suggest limited but significant contribution of
520 outer Solar System materials to the chondrite-forming regions. Interestingly, CV chondrites
521 may have accreted ¹⁷O- and ¹⁸O-rich water (i.e., $\Delta^{17}\text{O} > 15\text{‰}$) during their formation $\approx 1\text{My}$
522 before the more hydrated carbonaceous chondrites (Sugiura and Fujiya, 2014). It is possible
523 that inward radial mixing was more efficient at the time of CV chondrite accretion but
524 significantly decreased upon the formation of Jupiter, which limited later contribution of outer
525 water ices in favor of locally derived water in the accretion zones of carbonaceous asteroids.

526

527 **5- Concluding remarks**

528

529

530

We report the oxygen isotopic composition of sulfide- and magnetite-free, nearly pure
531 fayalite grains in CV chondrites Kaba and Mokoia. When combined with both the bulk and
532 matrix O-isotopic compositions of CV chondrites, their O-isotopic composition define the
533 continuous trend $\delta^{17}\text{O} = (0.84 \pm 0.03) \times \delta^{18}\text{O} - (4.25 \pm 0.1)$. This implies that the process
534 controlling the O-isotopic composition of the CV chondrite parent body was related to
535 isotopic equilibrium between ¹⁶O-rich anhydrous silicates and ¹⁷O- and ¹⁸O-rich fluid. Similar
536 behaviors are observed in CM, CR and CO chondrites, demonstrating the ubiquitous nature of
537 O-isotopic exchange as the main physical process controlling the O-isotopic features of
538 carbonaceous chondrites, regardless of the extent of alteration. Based on these results, we
539 estimate the abundance of water accreted by carbonaceous chondrites (quantified by the

540 water/rock ratio) to be CM (0.4) \geq CR (0.1–0.4) \geq CV (0.1–0.2) $>$ CO (0.01–0.10). This
541 suggests a heterogeneous distribution of water in the accretion zone of carbonaceous
542 asteroids. The relatively low water/rock ratios estimated for carbonaceous chondrites indicate
543 their accretion near the snowline, in the inner Solar System, as accretion further out in the
544 disk would have induced solar water/rock ratio of 1.2. Most of aqueously formed minerals in
545 carbonaceous chondrites show O-isotopic characteristics consistent with accretion of local
546 water, likely formed from the condensation of the gas near the snowline and/or liquid water
547 adsorbed at the grain surfaces. These results provide no evidence of carbonaceous chondrite
548 formation beyond the orbit of Jupiter and imply a limited influx of D- and ¹⁷O- and ¹⁸O-rich
549 water ice grains from the outer part of the Solar System. Such a limited influx might result
550 from a gap in the solar protoplanetary disk due to the early and rapid formation of Jupiter,
551 which would limit the inward motion of particles with size higher than 150 μm . This model
552 accounts for the O- and H-isotopic signatures of carbonaceous chondrites, and suggest their
553 accretion in the inner Solar System, closer to Jupiter than non-carbonaceous chondrites.
554 Hence, carbonaceous chondrites would have preferentially accreted W- and Mo-bearing
555 presolar grains crossing the orbit of Jupiter, resulting in significant lower W- and Mo-
556 anomalies in non-carbonaceous meteorites. Among carbonaceous chondrites, only CV
557 chondrites show O-isotopic features compatible with accretion of ¹⁷⁻¹⁸O-rich water, possibly
558 related to their older accretion age relative to other hydrated carbonaceous chondrites.

559

560 **Acknowledgments**

561

562 All of the data used in the present article are available by contacting Yves Marrocchi
563 (yvesm@crpg.cnrs-nancy.fr). Ludovic Ferrière and the National Museum History of Vienna
564 (Austria) are thanked for the loan of the Kaba and Mokoia sections. Matthieu Gounelle is
565 warmly thanked for helpful scientific discussions. Johan Villeneuve, Nordine Bouden, David

566 Madre and Andrey Gurenko are thanked for their assistance with isotopic measurements This
567 work was funded by l'Agence Nationale de la Recherche through grant ANR-14-CE33-0002-
568 01 SAPINS (PI Yves Marrocchi). We thanked three anonymous reviewers for constructive
569 comments and Associate Editor Frederic Moynier for careful editing. This is CRPG-CNRS
570 contribution #2517 and SAPINS contribution #10.

571 **Figure Caption**

572

573 **Fig. 1:** Back-scattered electron micrographs of fayalite grains in the Kaba CV chondrite.
574 (A) Fayalite grains located in the chondrule rim in association with iron sulfides and isolated
575 in the matrix. OA = opaque assemblage. (B) Sulfide- and magnetite-free fayalite grain
576 commonly observed in the Kaba and Mokoia matrices.

577

578 **Fig. 2:** Oxygen three-isotope plot for bulk and matrix CV chondrites (Clayton and Mayeda,
579 1999; 1984; Greenwood et al., 2010) and sulfide- and magnetite-free fayalite grains from
580 Mokoia and Kaba. Oxygen isotopic variations are expressed in delta units as deviations of the
581 $^{17}\text{O}/^{16}\text{O}$ and $^{18}\text{O}/^{16}\text{O}$ isotopic ratios relative to the V-SMOW international standard
582 ($\delta^x\text{O}=(^x\text{O}/^{16}\text{O}/^x\text{O}^{16}\text{O}_{\text{V-SMOW}}-1)\times 1000$; $x=^{18}\text{O}$ or ^{17}O). Two different lines (PCM = Primary
583 Chondrules Minerals and TFL) are shown (see text). The O-isotopic compositions of fayalite
584 in CV chondrite A-881317 (Doyle et al., 2015) and Kaba ((Krot and Nagashima, 2016),
585 corresponding to * in the figure caption) are also represented. CV water corresponds to the O-
586 isotopic composition from which fayalite grains have precipitated according to the
587 fractionation factor α (Zheng, 1993). Uncertainties shown are 2σ . (B) $\Delta^{17}\text{O}$ values (see text)
588 of bulk, matrix and fayalite in CV chondrites. The data are plotted arbitrarily along the x-axis.
589 Uncertainties shown are 2σ .

590

591 **Fig. 3:** (A) Oxygen three-isotope plot for bulk and matrix CV chondrites ((Clayton and
592 Mayeda, 1999; 1984)) and fayalite grains from Mokoia, Kaba and A-881317 (Doyle et al.,
593 2015). The O-isotopic composition of magnetite in Kaba chondrules (Marrocchi et al., 2016)
594 and in the matrix of A-881317 (Doyle et al., 2015) and Kaba (Krot and Nagashima, 2016) are
595 also represented. Uncertainties shown are 2σ . (B) $\Delta^{17}\text{O}$ values of bulk, matrix, fayalite and
596 magnetite in the CV chondrites Kaba, Mokoia and A881317. The similar $\Delta^{17}\text{O}$ observed
597 between fayalite and magnetite in A-881317 indicate that they probably formed at isotopic
598 equilibrium from the same fluid reservoir. To the contrary, fayalite and magnetite in Kaba
599 show significantly different $\Delta^{17}\text{O}$ that could be linked to the formation of magnetite during
600 the high-temperature chondrule-forming event (Marrocchi et al., 2016). Uncertainties shown
601 are 2σ .

602

603 **Fig. 4:** (A) Oxygen three-isotope plot of Ca-carbonates in CM chondrites Murchison and
604 Mighei (Lindgren et al., 2017). The O-isotopic compositions of Ca-carbonates define the
605 trend $\delta^{17}\text{O} = (0.70 \pm 0.03) \times \delta^{18}\text{O} - (5.65 \pm 1.25)$, similar, within errors, to that reported for 9
606 different CM chondrites (Verdier-Paoletti et al., 2017). The O-isotopic compositions of CM
607 alteration water inferred from direct measurements and mass balance calculations define a
608 continuous trend, parallel within errors to that shown by bulk CMs and Ca-carbonates, but
609 with a different intercept ($\delta^{17}\text{O} = (0.69 \pm 0.02) \times \delta^{18}\text{O} - (2.12 \pm 0.30)$). As both trends are
610 parallel, the temperature of carbonate precipitation can be determined (see text). Uncertainties
611 shown are 2σ . (B) $\Delta^{17}\text{O}$ values of inferred CM water showing the near terrestrial values of
612 water accreted by CM chondrites. Uncertainties shown are 2σ

613

614 **Fig. 5:** (A) Oxygen three-isotope plot of bulk, matrix and Ca-carbonates of CR chondrites
615 (Clayton and Mayeda, 1999; Jilly, 2015; Jilly et al., 2014; Schrader et al., 2011). The O-

616 isotopic compositions of CR alteration water from which Ca-carbonates precipitated are also
617 represented. CR water O-isotopic compositions were calculated based on the isotopic
618 equilibrium between Ca-carbonates and magnetite per CR chondrite (represented in panel (B);
619 data from Jilly, 2015). Uncertainties shown are 2σ .

620

621 **Fig. 6:** (A) Oxygen three-isotope plot of bulk and matrix in CO chondrites (Clayton and
622 Mayeda, 1999). The O-isotopic compositions of fayalite grains in CO-like MacAlpine Hills
623 88107 are also represented (Doyle et al., 2015). Together, the data define the continuous trend
624 with $\delta^{17}\text{O} = (0.68 \pm 0.08) \times \delta^{18}\text{O} - (4.08 \pm 0.14)$. CO water corresponds to the O-isotopic
625 composition from which fayalite grains precipitated according to the fractionation factor α
626 between fayalite and water (Zheng, 1993). Uncertainties shown are 2σ . (B) Oxygen isotopic
627 compositions of magnetite and fayalite in CO-like chondrite MacAlpine Hills 88107 (Doyle
628 et al., 2015) plot on a mass-dependent fractionation line, allowing the alteration temperature
629 and the O-isotopic composition of the alteration water of this chondrite to be determined (CO
630 water; see text for details). Uncertainties shown are 2σ .

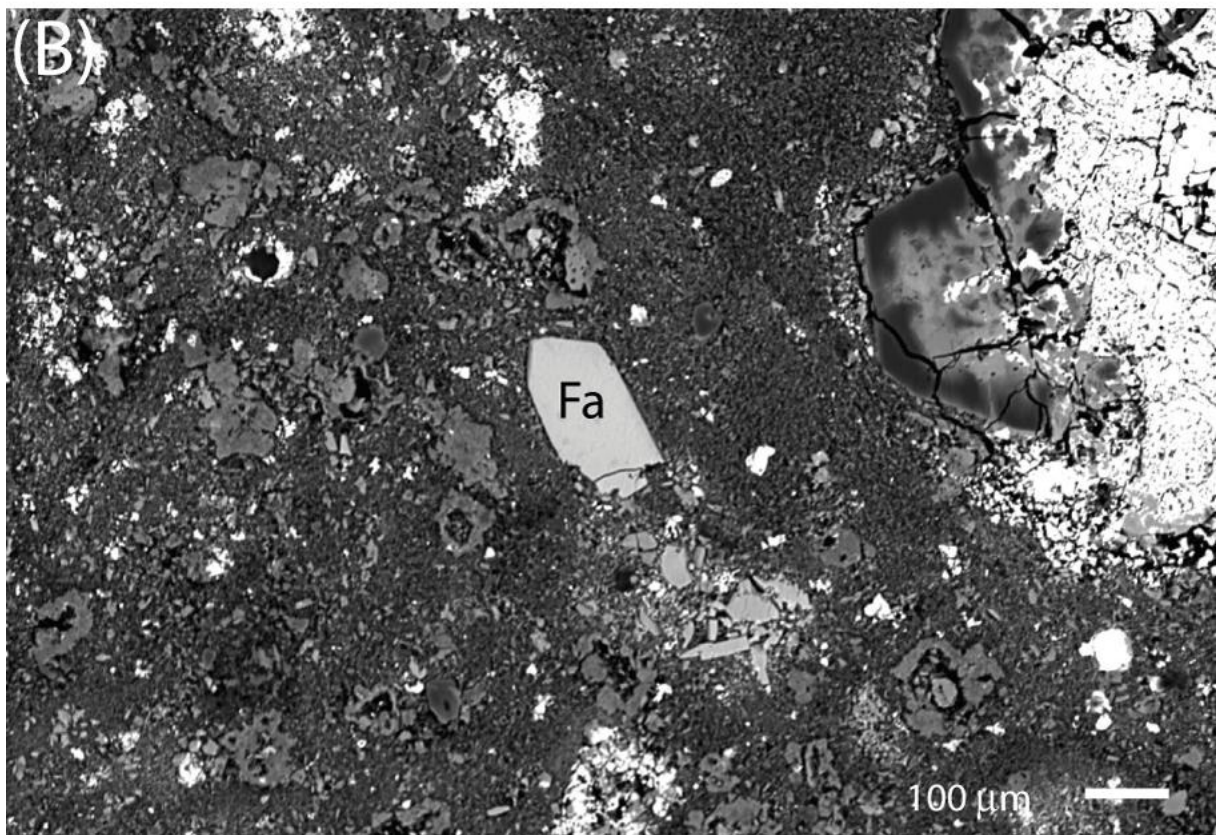
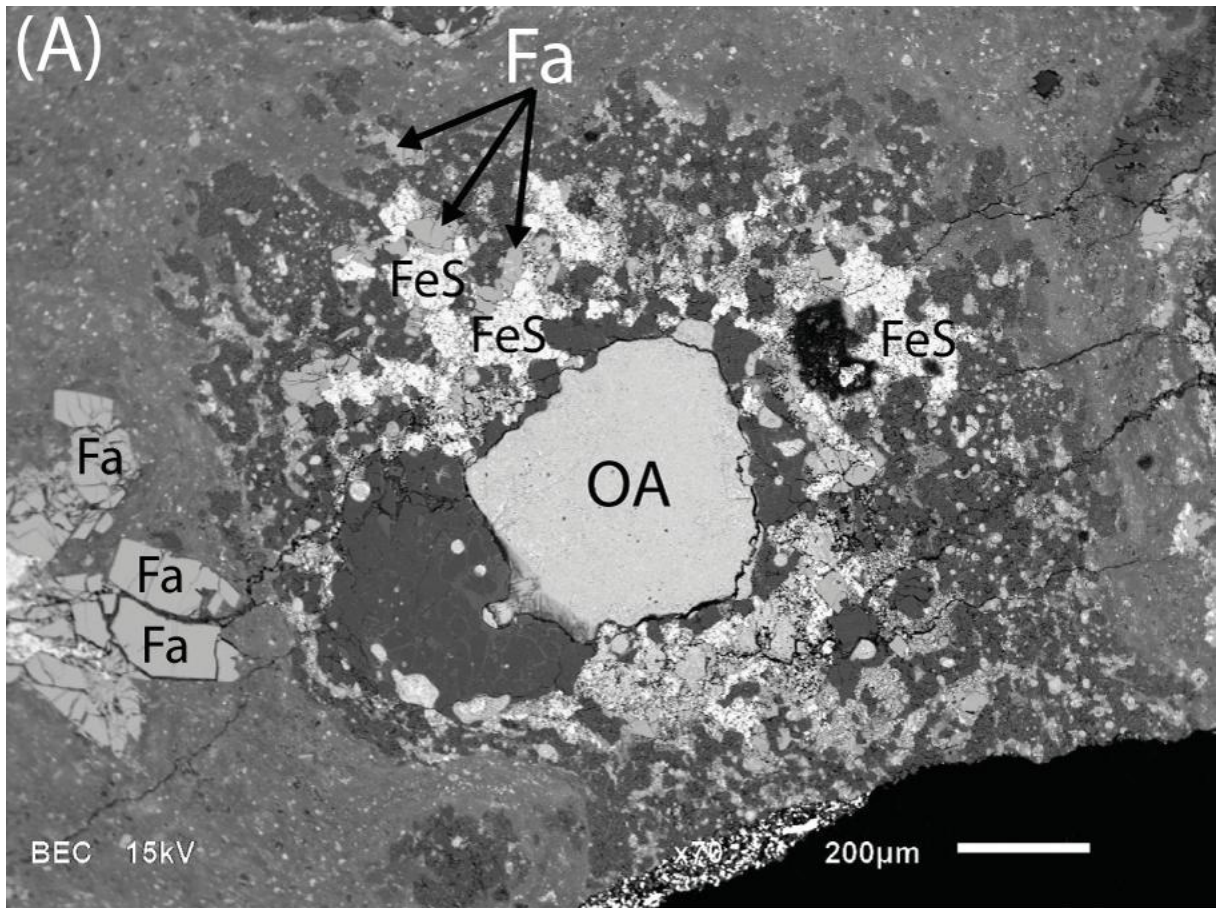
631

632 **Fig. 7:** Schematic representation of the water/rock ratio estimated for the CO, CV, CR and
633 CM chondrites.

634

635 **Fig. 8:** A) Coexistence and spatial separation of non-carbonaceous chondrite (NCC) and
636 carbonaceous chondrite (CC) reservoirs as depicted by (Kruijer et al., 2017). The early
637 formation of Jupiter (~ 1 Ma after the formation of the Solar System) would have acted as a
638 barrier against inward transport of solids across the disk, and thus mixing of the CC and NCC
639 reservoirs. (B) Key observables of the oxygen and hydrogen isotopic compositions in the
640 protoplanetary disk are at odds with the model proposed by (Kruijer et al., 2017).

641 (C) Scenario proposed herein for the preservation of ¹⁶O-rich and D-poor water in the inner
642 solar system. Jupiter would have acted as a barrier precluding significant inward transport of
643 outer Solar System water toward the inner Solar System. (D) Scenario proposed in this study
644 for the accretion of ¹⁶O-rich and D-poor water by hydrated carbonaceous asteroids. The
645 increasing water/rock ratios of CO, CV, CR and CM chondrites reflect that these different
646 types of carbonaceous asteroids accreted close to the snow line, at increasing heliocentric
647 distances.
648



649
650
651
652

Fig. 1

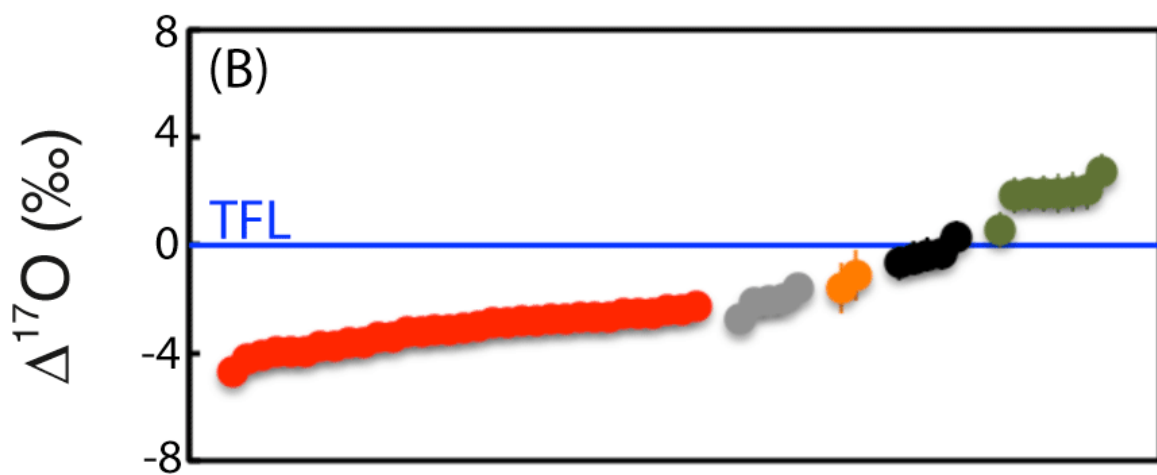
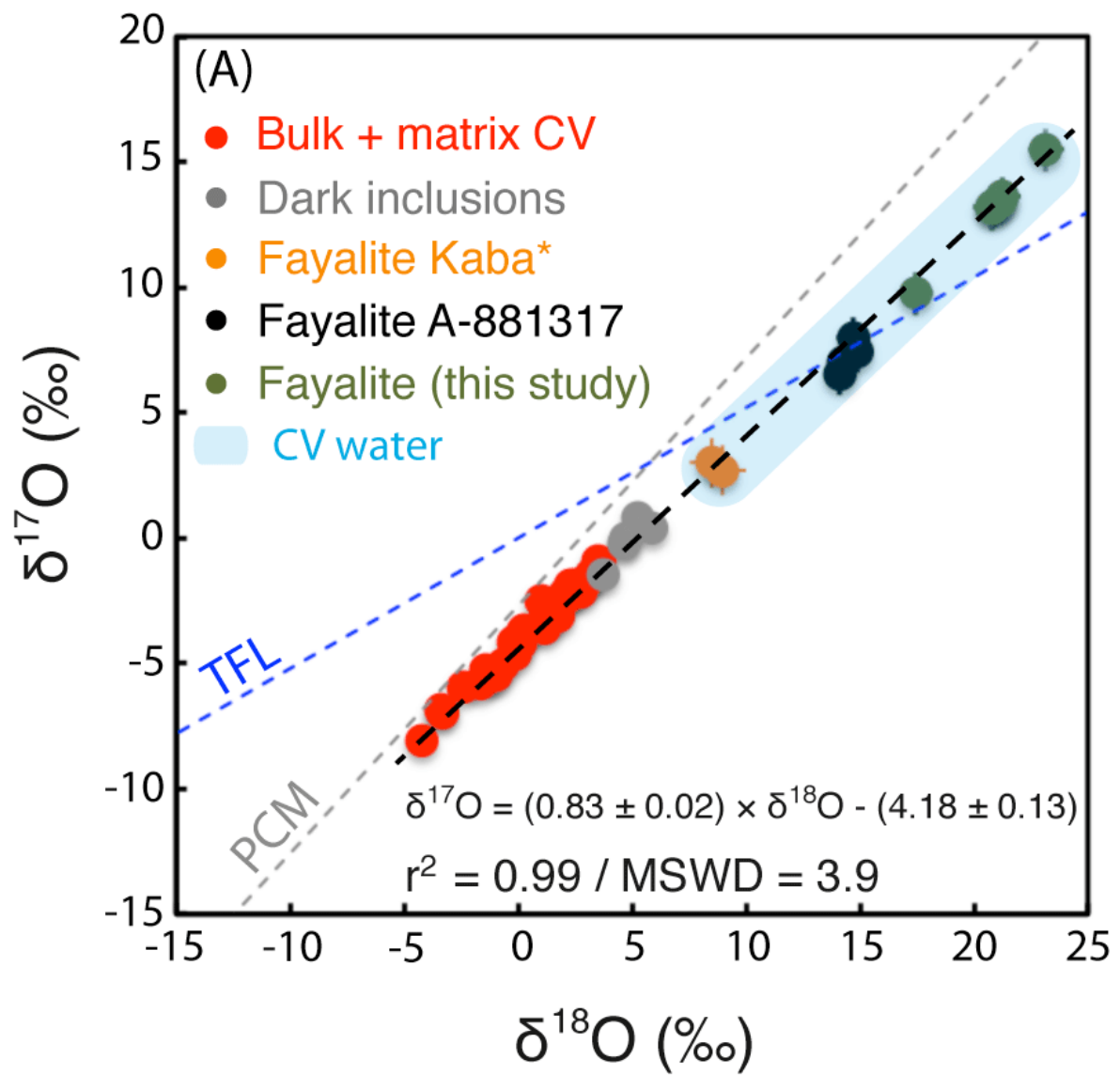


Fig. 2

653
 654
 655
 656
 657

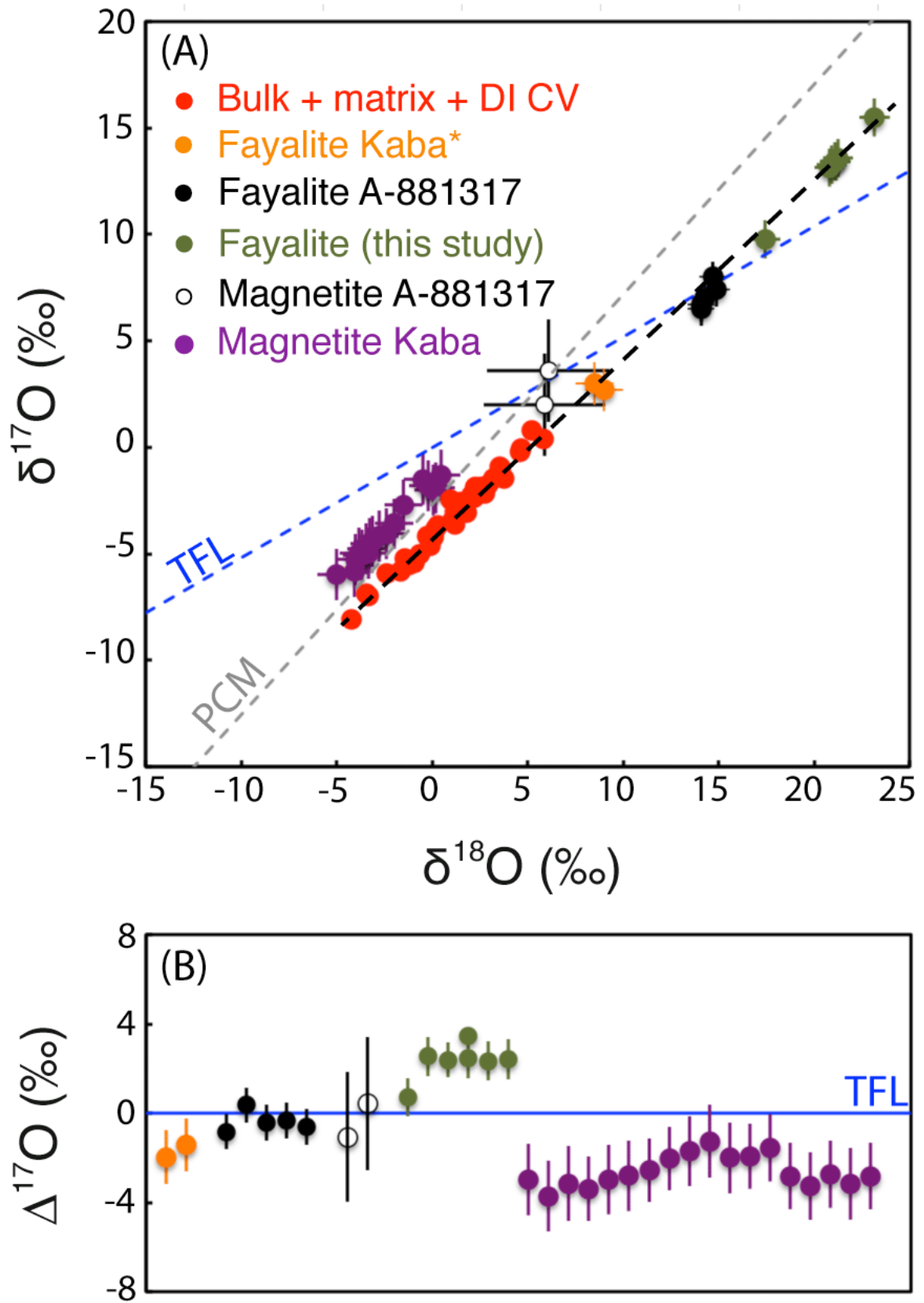


Fig. 3

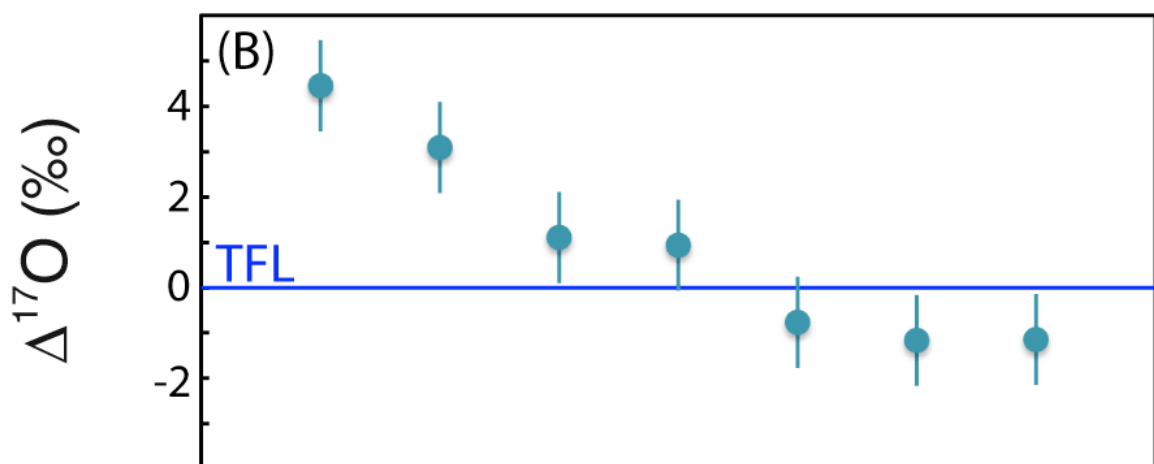
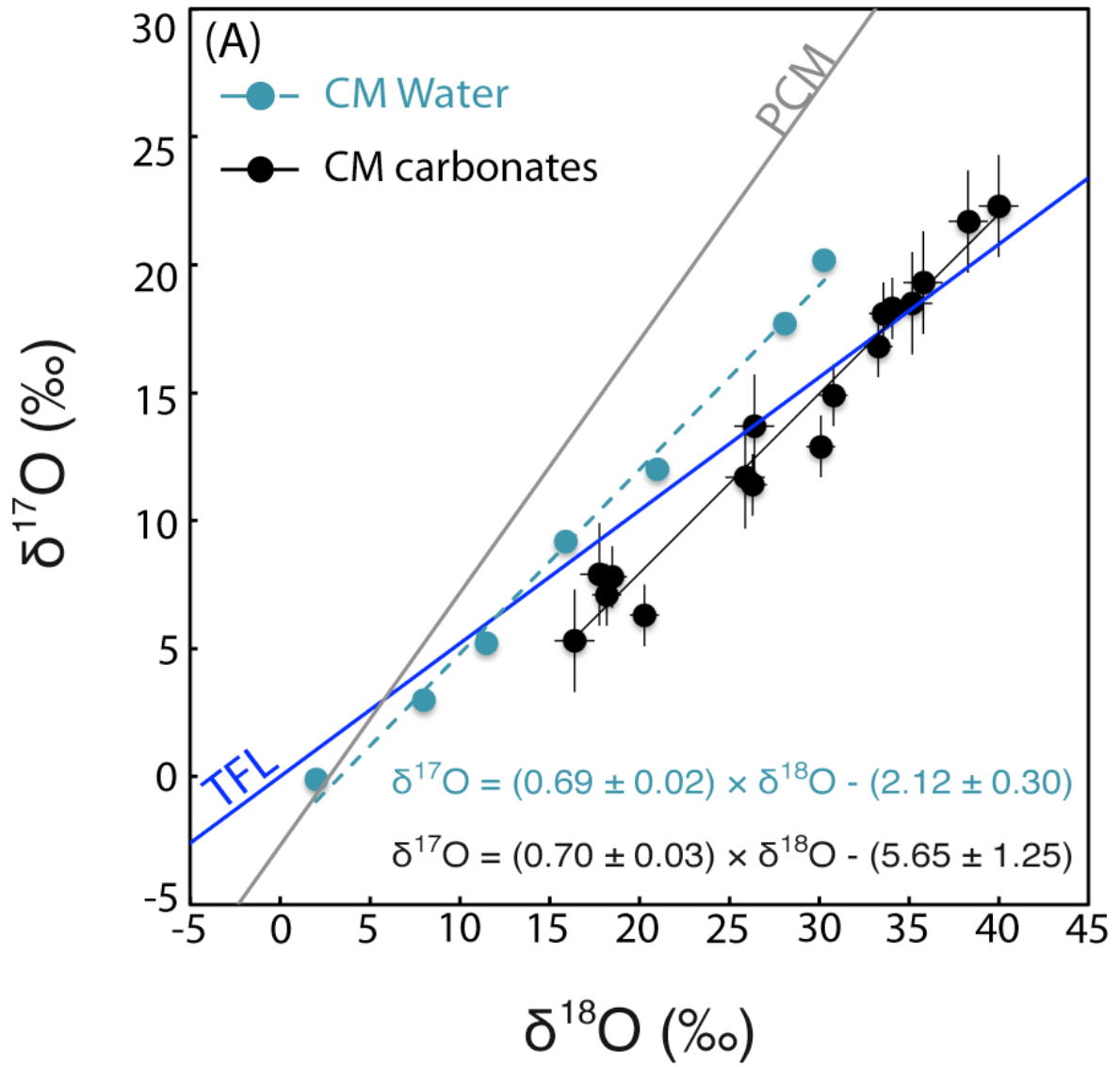
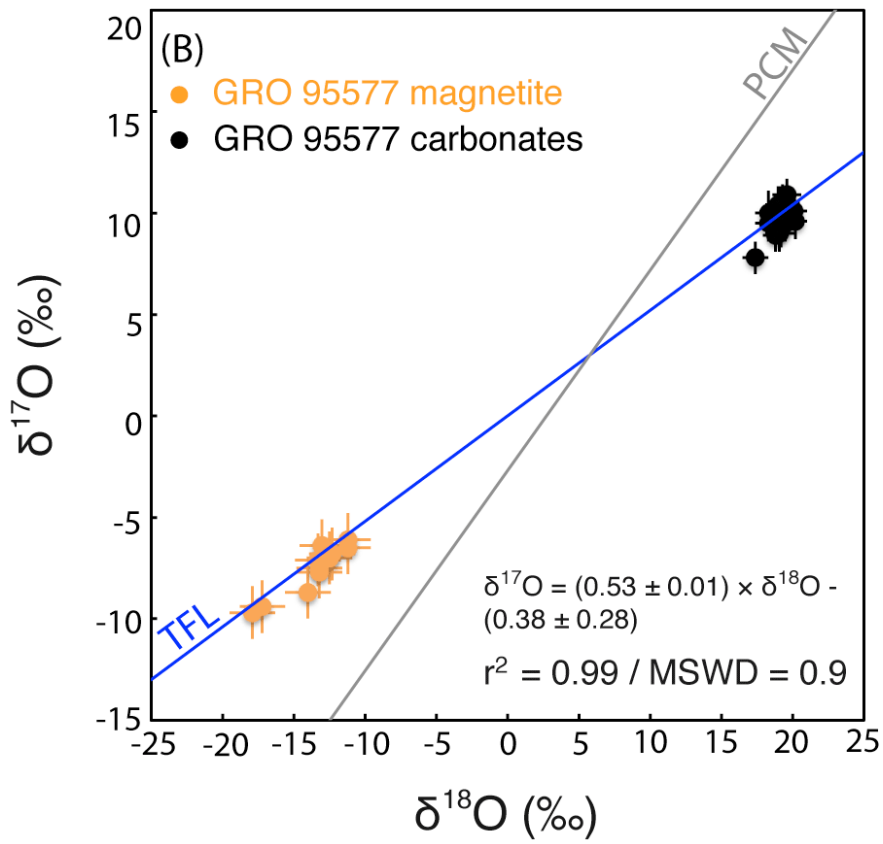
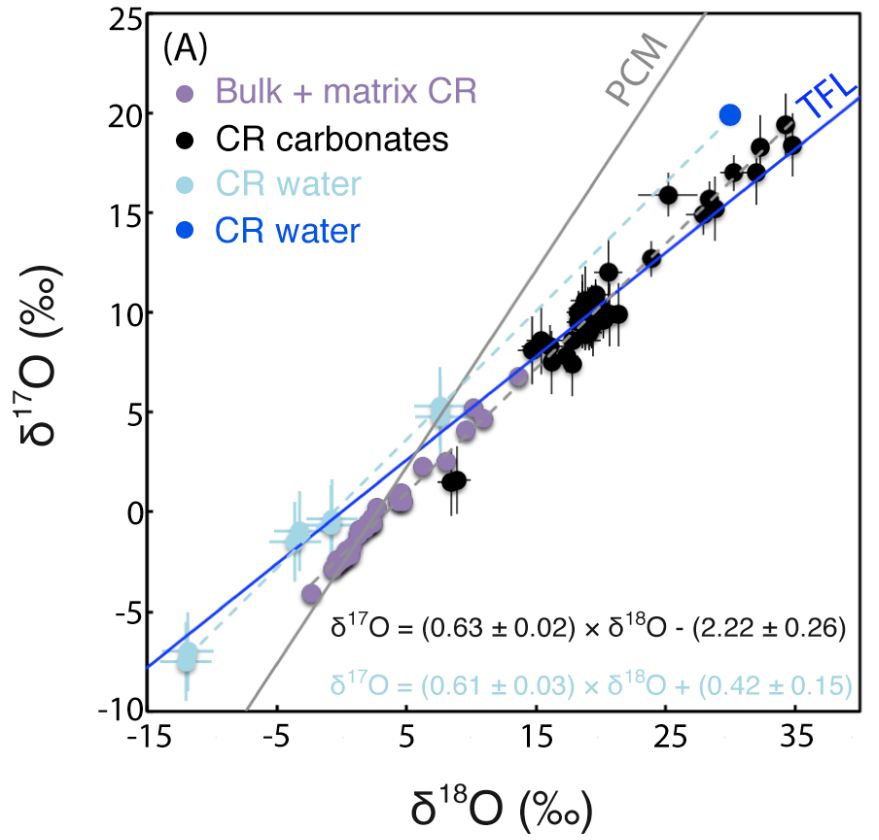


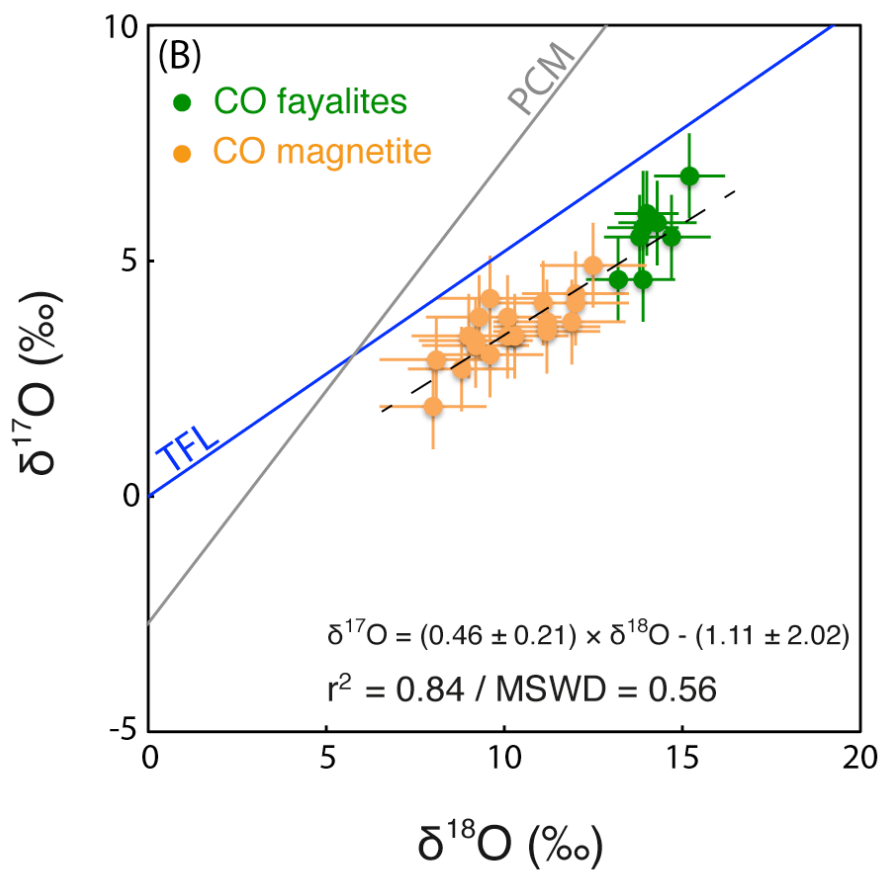
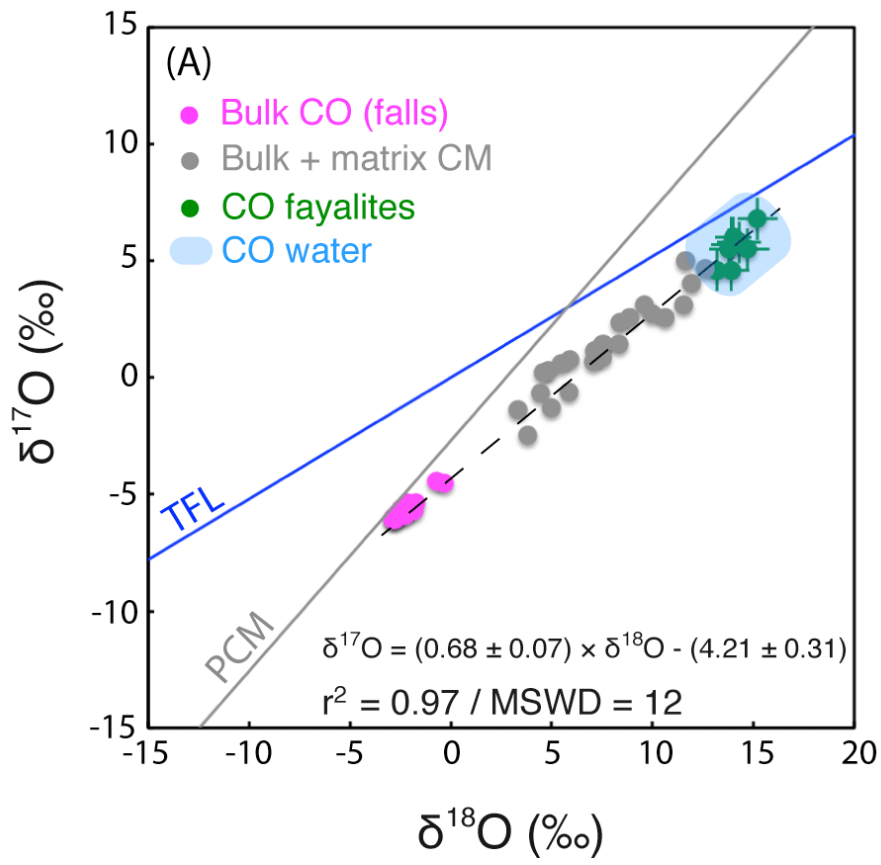
Fig. 4

661
662
663
664
665



666
667
668

Fig. 5



669
670

Fig. 6

671

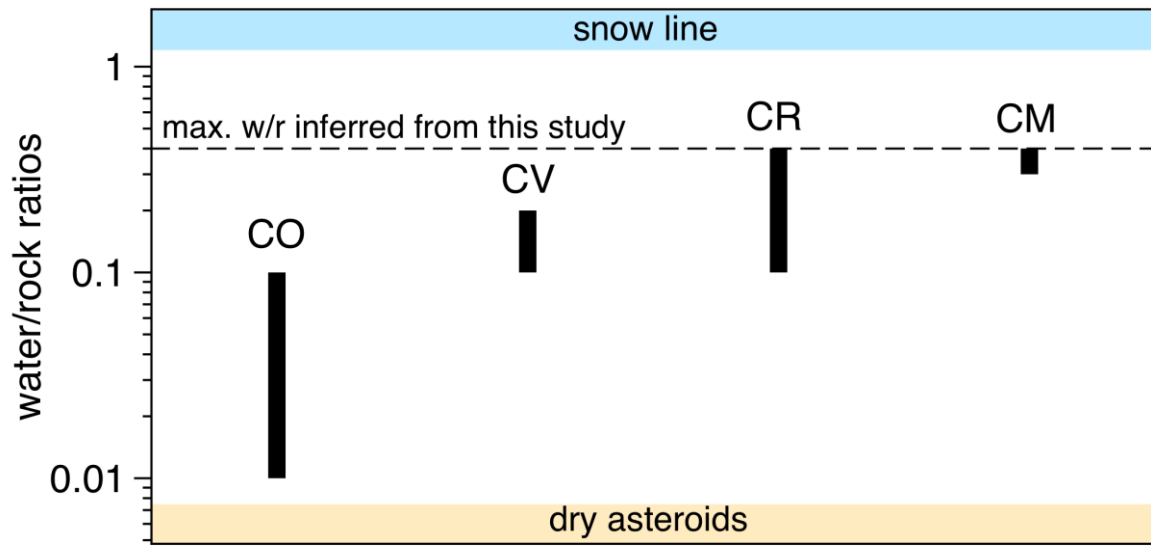
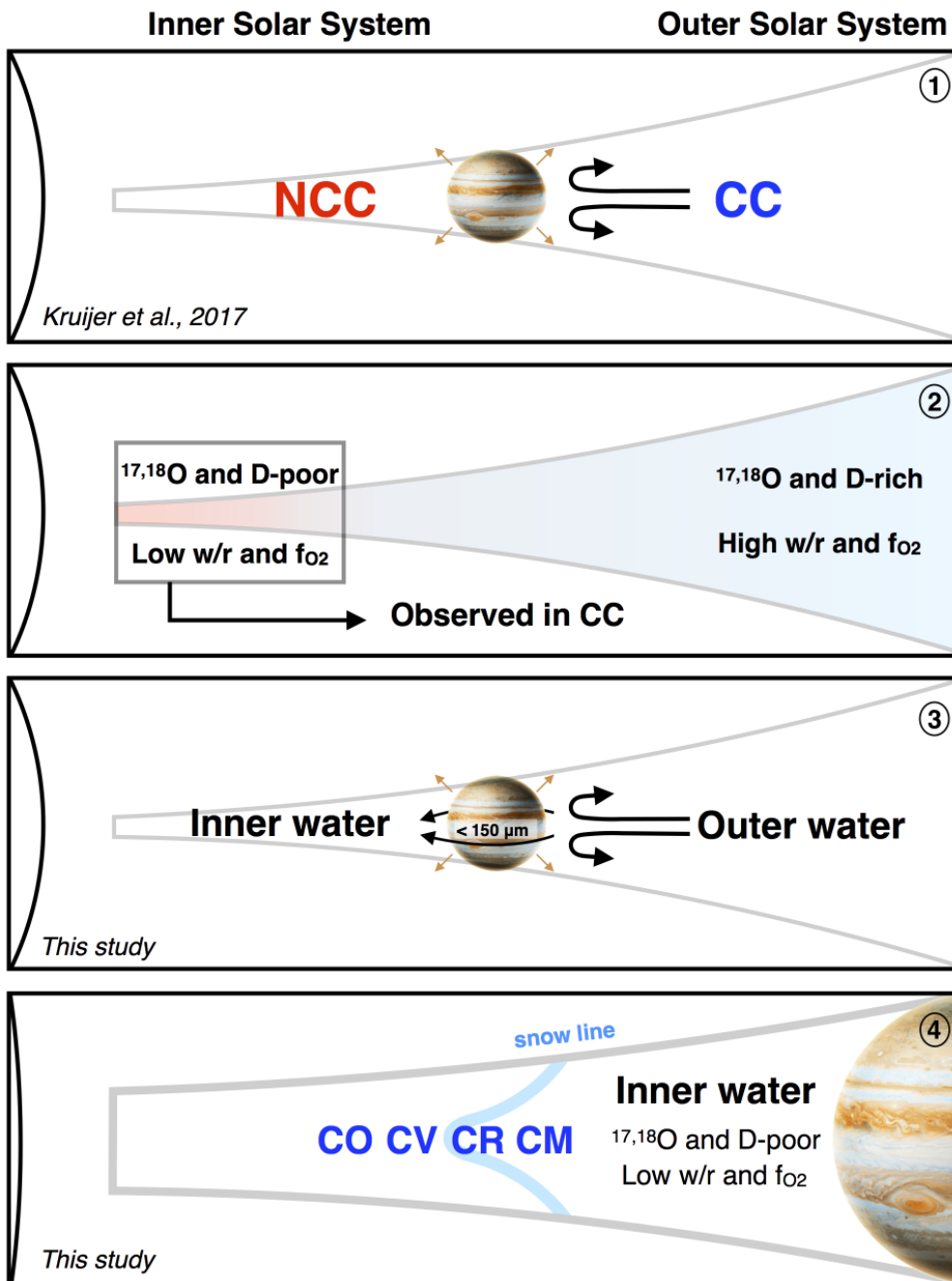


Fig. 7

672
673
674
675
676
677
678
679
680
681
682
683
684
685



686
687

Fig. 8

chondrite	point	SiO ₂	K ₂ O	FeO	Na ₂ O	Al ₂ O ₃	CaO	MnO	MgO	Cr ₂ O ₃	TiO ₂	Total	Fa
Kaba	Fa-1	29.3	bdl	69.1	bdl	bdl	bdl	0.7	0.8	bdl	bdl	99.9	98.9
	Fa-2	29.4	bdl	69.4	bdl	bdl	bdl	0.4	0.6	bdl	bdl	99.7	99.2
	Fa-3	29.2	bdl	69.2	bdl	bdl	bdl	0.7	0.5	bdl	bdl	99.7	99.2
	Fa-4	29.0	bdl	69.6	bdl	bdl	bdl	0.7	0.0	bdl	bdl	99.4	100.0
	Fa-5	29.8	bdl	67.1	bdl	bdl	bdl	0.8	2.1	bdl	bdl	99.7	97.0
	Fa-6	29.5	bdl	68.2	bdl	bdl	bdl	1.2	0.8	bdl	bdl	99.6	98.9
Mokoia	Fa-7	29.2	bdl	68.8	bdl	bdl	bdl	0.6	1.2	bdl	bdl	99.8	98.3
	Fa-8	28.9	bdl	68.1	bdl	bdl	bdl	0.9	1.8	bdl	bdl	99.7	97.4

Table 1: Chemical composition and Fa# of fayalite grains observed in the Kaba and Mokoia CV chondrites

chondrite	point	$\delta^{18}\text{O}$	2 σ	$\delta^{17}\text{O}$	2 σ	$\Delta^{17}\text{O}$	2 σ
Kaba	Fa-1	17.4	0.8	9.8	0.9	0.7	0.9
	Fa-2	21.3	0.8	13.6	0.9	2.5	0.9
	Fa-3	20.9	0.8	13.3	0.9	2.4	0.8
	Fa-4	21.1	0.8	13.4	0.9	2.5	0.9
	Fa-5	20.8	0.8	13.2	0.9	2.3	0.9
	Fa-6	21.2	0.8	13.4	0.9	2.4	0.9
Mokoia	Fa-7	23.2	0.8	15.5	0.9	3.5	0.8
	Fa-8	20.8	0.8	13.2	0.9	2.4	0.9

Table 2: Oxygen isotopic composition of fayalite grains in the Kaba and Mokoia CV chondrites. Uncertainties reported are 2 σ .

References

- Albarède, F., 2009. Volatile accretion history of the terrestrial planets and dynamic implications. *Nature* 461, 1227–1233. doi:10.1038/nature08477
- Alexander, C.M.O., 2017. The origin of inner Solar System water. *Philosophical Transactions of the Royal Society A: Mathematical, Physical and Engineering Sciences* 375, 20150384–20. doi:10.1098/rsta.2015.0384
- Alexander, C.M.O'D, Bowden, R., Fogel, M.L., Howard, K.T., Herd, C.D.K., Nittler, L.R., 2012. The Provenances of Asteroids, and Their Contributions to the Volatile Inventories of the Terrestrial Planets. *Science* 337, 721–723. doi:10.1126/science.1223474
- Alexander, C.M.O'D, Greenwood, R.C., Bowden, R., Gibson, J.M., Howard, K.T., Franchi, I.A., 2017. A multi-technique search for the most primitive CO chondrites. *Geochim. Cosmochim. Acta* 1–15. doi:10.1016/j.gca.2017.04.021
- Bitsch, B., Johansen, A., Lambrechts, M., Morbidelli, A., 2015. The structure of protoplanetary discs around evolving young stars. *A&A* 575, A28–17. doi:10.1051/0004-6361/201424964
- Bland, P.A., Jackson, M.D., Coker, R.F., Cohen, B.A., Webber, J.B.W., Lee, M.R., Duffy, C.M., Chater, R.J., Ardakani, M.G., McPhail, D.S., McComb, D.W., Benedix, G.K., 2009. Why aqueous alteration in asteroids was isochemical: High porosity ≠ high permeability. *Earth Planet. Sci. Lett.* 287, 559–568. doi:10.1016/j.epsl.2009.09.004
- Bonal, L., Quirico, E., Bourot-Denise, M., Montagnac, G., 2006. Determination of the petrologic type of CV3 chondrites by Raman spectroscopy of included organic matter. *Geochim. Cosmochim. Acta* 70, 1849–1863. doi:10.1016/j.gca.2005.12.004
- Brearley, A.J., 2006. The action of water. Meteorites and the early solar system II. Edited by Lauretta D. S. and McSween H. Y. Tucson, Arizona: The University of Arizona Press. pp. 587–624.
- Chacko, T., Cole, D.R., Horita, J., 2001. Equilibrium Oxygen, Hydrogen and Carbon Isotope Fractionation Factors Applicable to Geologic Systems. *Reviews in Mineralogy and Geochemistry* 43, 1–81. doi:10.2138/gsrmg.43.1.1
- Choi, B.-G., Krot, A.N., Wasson, J.T., 2000. Oxygen isotopes in magnetite and fayalite in CV chondrites Kaba and Mokoia. *Meteoritics & Planetary Science* 35, 1239–1248. doi:10.1111/j.1945-5100.2000.tb01512.x
- Clayton, R.N., Grossman, L., Mayeda, T.K., 1973. A Component of Primitive Nuclear Composition in Carbonaceous Meteorites. *Science* 182, 485–488. doi:10.1126/science.182.4111.485
- Clayton, R.N., Mayeda, T.K., 1999. Oxygen isotope studies of carbonaceous chondrites. *Geochim. Cosmochim. Acta* 63, 2089–2104. doi:10.1016/s0016-7037(99)00090-3
- Clayton, R.N., Mayeda, T.K., 1984. The oxygen isotope record in Murchison and other carbonaceous chondrites. *Earth and Planetary Science Letters* 67, 151–161. doi:10.1016/0012-821x(84)90110-9
- Doyle, P.M., Jogo, K., Nagashima, K., Krot, A.N., Wakita, S., Ciesla, F.J., Hutcheon, I.D., 2015. Early aqueous activity on the ordinary and carbonaceous chondrite parent bodies recorded by fayalite. *Nat Comms* 6, 7444. doi:10.1038/ncomms8444
- Garenne, A., Beck, P., Montes-Hernandez, G., Chiriach, R., Toche, F., Quirico, E., Bonal, L., Schmitt, B., 2014. The abundance and stability of “water” in type 1 and 2 carbonaceous chondrites (CI, CM and CR). *Geochim. Cosmochim. Acta* 137, 93–112. doi:10.1016/j.gca.2014.03.034
- Greenwood, R.C., Franchi, I.A., 2004. Alteration and metamorphism of CO3 chondrites: Evidence from oxygen and carbon isotopes. *Meteoritics & Planetary Science* 39, 1823–1838. doi:10.1111/j.1945-5100.2004.tb00078.x

- Greenwood, R.C., Franchi, I.A., Kearsley, A.T., Alard, O., 2010. The relationship between CK and CV chondrites. *Geochim. Cosmochim. Acta* 74, 1684–1705. doi:10.1016/j.gca.2009.11.029
- Gundlach, B., Blum, J., 2015. The stickiness of micrometer-sized water-ice particles. *The Astrophys. J.* 798, 34–42. doi:10.1088/0004-637X/798/1/34
- Güttler, C., Blum, J., Zsom, A., Ormel, C.W., Dullemond, C.P., 2010. The outcome of protoplanetary dust growth: pebbles, boulders, or planetesimals? *A&A* 513, A56–16. doi:10.1051/0004-6361/200912852
- Hartmann, L., Calvet, N., Gullbring, E., D'Alessio, P., 1998. Accretion and the Evolution of T-Tauri Disks. *The Astrophysical Journal*. 495, 385–400. doi:10.1086/305277
- Hewins, R.H., Bourot-Denise, M., Zanda, B., Leroux, H., Barrat, J.-A., Humayun, M., Göpel, C., Greenwood, R.C., Franchi, I.A., Pont, S., Lorand, J.-P., Cournède, C., Gattacceca, J., Rochette, P., Kuga, M., Marrocchi, Y., Marty, B., 2014. The Paris meteorite, the least altered CM chondrite so far. *Geochim. Cosmochim. Acta* 124, 190–222. doi:10.1016/j.gca.2013.09.014
- Hua, X., Buseck, P.R., 1995. Fayalite in the Kaba and Mokoia carbonaceous chondrites. *Geochim. Cosmochim. Acta* 59, 563–578. doi:10.1016/0016-7037(94)00383-w
- Jacquet, E., Robert, F., 2013. Water transport in protoplanetary disks and the hydrogen isotopic composition of chondrites. *Icarus* 223, 722–732. doi:10.1016/j.icarus.2013.01.022
- Jilly, C.E., 2015. Timescales and conditions for the aqueous alteration of chondrites. Dissertation of the university of hawai'i.
- Jilly, C.E., Huss, G.R., Nagashima, K., 2014. Oxygen isotope fractionation among secondary calcite and magnetite in CR chondrites. 45th Lunar and Planetary Science Conference, Houston, USA. Abstract # 1642.
- Jogo, K., Nakamura, T., Noguchi, T., Zolotov, M.Y., 2009. Fayalite in the Vigarano CV3 carbonaceous chondrite: Occurrences, formation age and conditions. *Earth and Planetary Science Letters* 287, 320–328. doi:10.1016/j.epsl.2009.08.014
- Krot, A.N., Brearley, A.J., Petaev, M.I., Kallemeyn, G.W., Sears, D.W.G., Benoit, P.H., Hutcheon, I.D., Zolensky, M.E., Keil, K., 2000. Evidence for low- temperature growth of fayalite and hedenbergite in MacAlpine Hills 88107, an ungrouped carbonaceous chondrite related to the CM- CO clan. *Meteoritics & Planetary Science* 35, 1365–1386. doi:10.1111/j.1945-5100.2000.tb01522.x
- Krot, A.N., Nagashima, K., 2016. Evidence for oxygen-isotope exchange in chondrules and refractory inclusions during fluid-rock interaction on the CV chondrite parent body. 79th Annual Meeting of the Meteoritical Society, Berlin, Germany. LPI Contribution No. 1921, id.6014
- Krot, A.N., Nagashima, K., Alexander, C.M.O'D, Ciesla, F.J., Fujiya, W., Bonal, L., 2015. Sources of Water and Aqueous Activity on the Chondrite Parent Asteroids, in: *Asteroids IV*. University of Arizona Press, pp. 1–27. doi:10.2458/azu_uapress_9780816532131-ch033
- Kruijer, T.S., Burkhardt, C., Budde, G., Kleine, T., 2017. Age of Jupiter inferred from the distinct genetics and formation times of meteorites. *Proceedings of the National Academy of Sciences* 201704461. doi:10.1073/pnas.1704461114
- Le Guillou, C., Brearley, A., 2014. Relationships between organics, water and early stages of aqueous alteration in the pristine CR3.0 chondrite MET 00426. *Geochim. Cosmochim. Acta* 131, 344–367. doi:10.1016/j.gca.2013.10.024
- Lindgren, P., Lee, M.R., Starkey, N.A., Franchi, I.A., 2017. Fluid evolution in CM carbonaceous chondrites tracked through the oxygen isotopic compositions of carbonates.

- Geochim. Cosmochim. Acta 204, 240–251. doi:10.1016/j.gca.2017.01.048
- Lodders, K., 2003. Solar system abundances and condensation temperatures of the elements. *Astrophys. J.* 591, 1220–1247. doi:10.1086/375492
- Marrocchi, Y., Chaussidon, M., Piani, L., Libourel, G., 2016. Early scattering of the solar protoplanetary disk recorded in meteoritic chondrules. *Science Advances* 2, e1601001–e1601001. doi:10.1126/sciadv.1601001
- Marrocchi, Y., Libourel, G., 2013. Sulfur and sulfides in chondrules. *Geochim. Cosmochim. Acta* 119, 117–136. doi:10.1016/j.gca.2013.05.020
- Marty, B., 2012. The origins and concentrations of water, carbon, nitrogen and noble gases on Earth. *Earth Planet. Sci. Lett.* 313–314, 56–66. doi:10.1016/j.epsl.2011.10.040
- Morbidelli, A., Bitsch, B., CRIDA, A., Gounelle, M., Guillot, T., Jacobson, S., Johansen, A., Lambrechts, M., Lega, E., 2016. Fossilized condensation lines in the Solar System protoplanetary disk. *Icarus* 267, 368–376. doi:10.1016/j.icarus.2015.11.027
- Morlok, A., Libourel, G., 2013. Aqueous alteration in CR chondrites: Meteorite parent body processes as analogue for long-term corrosion processes relevant for nuclear waste disposal. *Geochim. Cosmochim. Acta* 103, 76–103. doi:10.1016/j.gca.2012.10.030
- Oka, A., Nakamoto, T., Ida, S., 2011. Evolution of snowline in optically thick protoplanetary disks: Effects of water ice opacity and dust grain size. *Astrophys. J.* 738, 141–11. doi:10.1088/0004-637X/738/2/141
- Piani, L., Robert, F., Beyssac, O., Binet L., Bourot-Denise, M., Derenne, S., Guillou, C.L., Marrocchi, Y., Mostefaoui, S., Rouzard, J.-N., Thomen, A., 2011. Structure, composition, and location of organic matter in the enstatite chondrite Sahara 97096 (EH3). *Meteoritics & Planetary Science* 47, 8–29. doi:10.1111/j.1945-5100.2011.01306.x
- Piani, L., Robert, F., Remusat, L., 2015. Micron-scale D/H heterogeneity in chondrite matrices: A signature of the pristine solar system water? *Earth Planet. Sci. Lett.* 415, 154–164. doi:10.1016/j.epsl.2015.01.039
- Piani, L., Yurimoto, H., Remusat, L., 2017. A Dual Origin for Water in the CM Carbonaceous Chondrites. 48th Lunar and Planetary Science Conference, Houston, USA. Abstract # 1203.
- Ros, K., Johansen, A., 2013. Ice condensation as a planet formation mechanism. *A&A* 552, A137–14. doi:10.1051/0004-6361/201220536
- Sakamoto, N., Seto, Y., Itoh, S., Kuramoto, K., Fujino, K., Nagashima, K., Krot, A.N., Yurimoto, H., 2007. Remnants of the Early Solar System Water Enriched in Heavy Oxygen Isotopes. *Science* 317, 231–233. doi:10.1126/science.1142021
- Schrader, D.L., Davidson, J., 2017. CM and CO chondrites: A common parent body or asteroidal neighbors? Insights from chondrule silicates. *Geochim. Cosmochim. Acta* 214, 157–171. doi:10.1016/j.gca.2017.07.031
- Schrader, D.L., Franchi, I.A., Connolly, H.C., Jr, Greenwood, R.C., Lauretta, D.S., Gibson, J.M., 2011. The formation and alteration of the Renazzo-like carbonaceous chondrites I: Implications of bulk-oxygen isotopic composition. *Geochim. Cosmochim. Acta* 75, 308–325. doi:10.1016/j.gca.2010.09.028
- Seto, Y., Sakamoto, N., Fujino, K., Kaito, T., Oikawa, T., Yurimoto, H., 2008. Mineralogical characterization of a unique material having heavy oxygen isotope anomaly in matrix of the primitive carbonaceous chondrite Acfer 094. *Geochim. Cosmochim. Acta* 72, 2723–2734. doi:10.1016/j.gca.2008.03.010
- Sugiura, N., Fujiya, W., 2014. Correlated accretion ages and ϵ ⁵⁴Cr of meteorite parent bodies and the evolution of the solar nebula. *Meteorit Planet Sci* 49, 772–787. doi:10.1111/maps.12292
- Vacher, L.G., Marrocchi, Y., Verdier-Paoletti, M.J., Villeneuve, J., Gounelle, M., 2016. Inward radial mixing of interstellar water ices in the Solar protoplanetary disk. *The*

- Astrophysical Journal Letters 827, 1–6. doi:10.3847/2041-8205/827/1/L1
- Vacher, L.G., Marrocchi, Y., Villeneuve, J., Verdier-Paoletti, M.J., Gounelle, M., 2017. Petrographic and C & O isotopic characteristics of the earliest stages of aqueous alteration of CM chondrites. *Geochim. Cosmochim. Acta* 213, 271–290. doi:10.1016/j.gca.2017.06.049
- Verdier-Paoletti, M.J., Marrocchi, Y., Avice, G., Roskosz, M., Gurenko, A., Gounelle, M., 2017. Oxygen isotope constraints on the alteration temperatures of CM chondrites. *Earth Planet. Sci. Lett.* 458, 273–281. doi:10.1016/j.epsl.2016.10.055
- Walsh, K.J., Morbidelli, A., Raymond, S.N., O'Brien, D.P., Mandell, A.M., 2011. A low mass for Mars from Jupiter's early gas-driven migration. *Nature* 475, 206–209. doi:10.1038/nature10201
- Yang, L., Ciesla, F.J., Lyons, J.R., Lee, J.E., 2011. Oxygen isotope anomalies in the solar nebula inherited from the proto-solar cloud. 42th Lunar and Planetary Science Conference, Houston, USA. Abstract # 1602.
- Young, E.D., Ash, R.D., England, P., Rumble, D., 1999. Fluid Flow in Chondritic Parent Bodies: Deciphering the Compositions of Planetesimals. *Science* 286, 1331–1335. doi:10.1126/science.286.5443.1331
- Yurimoto, H., Itoh, S., Zolensky, M., Kusakabe, M., Karen, A., Bodnar, R., 2014. Isotopic compositions of asteroidal liquid water trapped in fluid inclusions of chondrites. *GEOCHEMICAL JOURNAL* 48, 549–560. doi:10.2343/geochemj.2.0335
- Yurimoto, H., Kuramoto, K., 2004. Molecular cloud origin for the oxygen isotope heterogeneity in the solar system. *Science* 305, 1763–1766. doi:10.1126/science.1100989
- Zheng, Y.F., 1993. Calculation of oxygen isotope fractionation in anhydrous silicate minerals. *Geochim. Cosmochim. Acta* 57, 1079–1091. doi:10.1016/0016-7037(93)90042-u
- Zhu, Z., Nelson, R.P., Dong, R., Espaillat, C., Hartmann, L., 2012. Dust filtration by planet-induced gap edges: Implications for transitional disks. *Astrophys. J.* 755, 6–18. doi:10.1088/0004-637X/755/1/6
- Zolensky, M., Barrett, R., Browning, L., 1993. Mineralogy and composition of matrix and chondrule rims in carbonaceous chondrites. *Geochim. Cosmochim. Acta* 57, 3123–3148. doi:10.1016/0016-7037(93)90298-b
- Zolensky, M.E., Bodnar, R.J., Yurimoto, H., Itoh, S., Fries, M., Steele, A., Chan, Q.H.S., Tsuchiyama, A., Kebukawa, Y., Ito, M., 2017. The search for and analysis of direct samples of early Solar System aqueous fluids. *Philosophical Transactions of the Royal Society A: Mathematical, Physical and Engineering Sciences* 375, 20150386. doi:10.1098/rsta.2015.0386
- Zolensky, M.E., Mittlefehldt, D.W., Lipschutz, M.E., 1997. CM chondrites exhibit the complete petrologic range from type 2 to 1. *Geochim. Cosmochim. Acta* 61, 5099–5115. doi:10.1016/s0016-7037(97)00357-8
- Zolotov, M.Y., Mironenko, M.V., Shock, E.L., 2006. Thermodynamic constraints on fayalite formation on parent bodies of chondrites. *Meteoritics & Planetary Science* 41, 1775–1796. doi:10.1111/j.1945-5100.2006.tb00451.x